

Density Fluctuation Mediated Superconductivity

P. Monthoux and G.G. Lonzarich

Cavendish Laboratory, University of Cambridge

Madingley Road, Cambridge CB3 0HE, United Kingdom

(October 30, 2018)

Abstract

We compare predictions of the mean-field theory of superconductivity for metallic systems on the border of a density instability for cubic and tetragonal lattices. The calculations are based on the parameterisation of an effective interaction arising from the exchange of density fluctuations and assume that a single band is relevant for superconductivity. The results show that for comparable model parameters, density fluctuation mediated pairing is more robust in quasi-two dimensions than in three dimensions, and that the robustness of pairing increases gradually as one goes from a cubic structure to a more and more anisotropic tetragonal structure. We also find that the robustness of density fluctuation mediated pairing can depend sensitively on the incipient ordering wavevector. We discuss the similarities and differences between the mean-field theories of superconductivity for density mediated and magnetically mediated pairing.

PACS Nos. 74.20.Mn

Typeset using REVTeX

I. INTRODUCTION

Soon after the development of the BCS [1] theory of superconductivity it was realized that Cooper instabilities could arise not only from the exchange of phonons, but also from overscreening of the Coulomb interaction in a model Fermi liquid without ion dynamics. Due to the sharpness of the Fermi surface, the generalized spin and charge susceptibilities exhibit Friedel oscillations in space. Kohn and Luttinger [2] argued that oscillations of a similar origin can show up in the effective interaction between quasiparticles. Keeping all diagrams up to second order in a model bare fermion-fermion interaction, they also found an induced attraction which does not rely on the presence of the Friedel oscillations. They demonstrated that it was possible in principle to construct an anisotropic Cooper state that sampled mainly the attractive regions of the effective pairing interaction.

The Kohn-Luttinger model applies where the susceptibilities or response functions are adequately represented by the bare Lindhard function for a homogeneous electron gas for which the oscillations are weak and hence the calculated superconducting transition temperatures T_c turn out to be typically well below the experimentally accessible range. As a charge or spin instability is approached, however, we expect the corresponding response function and its real space attractive regions to become enhanced. Provided that it is possible to match the Cooper pair state to the attractive regions, T_c may rise to the experimentally accessible range. An extension of the Kohn-Luttinger theory would naturally lead to spin dependent quasiparticle interactions. Current models of magnetically mediated superconductivity focus on such magnetic interactions which are expected to dominate on the border of magnetic long-range order.

It has been shown that this magnetic interaction treated at the mean-field level can produce anomalous normal state properties and superconducting instabilities to anisotropic pairing states. It correctly predicted the symmetry of the Cooper state in the copper oxide superconductors [3] and is consistent with spin-triplet p-wave pairing in superfluid 3He [for a recent review see, e.g., ref. [4]]. One also gets the correct order of magnitude of

the superconducting and superfluid transition temperature T_c when the model parameters are inferred from experiments in the normal state of the above systems. There is growing evidence that the magnetic interaction model may be relevant to other materials on the border of magnetism.

In our previous work [5–7] we focussed on clarifying the general features of the magnetic interaction model. The latter may be relevant to understanding the superconductivity recently discovered, for example, on the border of antiferromagnetism in systems such as cubic $CeIn_3$ [8] and its tetragonal counterpart $CeRhIn_5$ [9] and on the border of ferromagnetism in UGe_2 [10], $URhGe$ [11] and $ZrZn_2$ [12].

In contrast to the conventional phonon-mediated interaction, which is usually taken to be local in space but non-local in time, the magnetic interaction is non-local in both space and time. The non-locality in space leads to anisotropic pairing states whose nature can be acutely sensitive to details of the lattice and electronic structure, and the form of the quasiparticle interaction. For simplicity, in references [5–7] we considered only a simple cubic or tetragonal crystal structure, a single tight-binding energy band and a magnetic interaction treated at the mean-field level.

One crucial aspect of the magnetic interaction is the vector nature of the spin degree of freedom. At first sight it might appear that the longitudinal and transverse phonons that mediate the usual lattice interaction would be analogous to the longitudinal and transverse spin fluctuations that mediate the magnetic interaction. However, the latter interaction depends on the relative spin orientation of the interacting particles and hence has a different sign and magnitude for the spin-singlet and spin-triplet Cooper states. By contrast, the conventional phonon mediated interaction is oblivious to the spin degree of freedom of the quasiparticles.

One of the consequences is that on the border of ferromagnetism, the magnetic interaction is typically only attractive in the spin-triplet channel. In that case, only the longitudinal spin fluctuations contributing to pairing while all three contribute to the self-interaction that tends to be pair breaking. This disadvantage can be mitigated in systems with strong mag-

netic anisotropy in that the effect of the transverse spin fluctuations on the self-interaction would be suppressed while the strength of the pairing interaction arising from longitudinal spin fluctuations need not be reduced. By contrast to isotropic magnetic pairing in the spin-triplet channel, in conventional phonon mediated superconductivity and in magnetic pairing in the spin-singlet channel, all modes contribute both to the pairing and to the self-interaction effects.

We have also found that for the model considered in references [5–7] the robustness of magnetic pairing increases gradually as one goes from a cubic to a more and more anisotropic tetragonal structure under otherwise similar conditions. This is due to the increase with growing anisotropy of the density of states of both the quasiparticles and of the magnetic fluctuations that mediate the quasiparticle interaction. One expects and calculations presented in this paper show that this result carries over to other pairing mechanisms treated at the same level of approximation as in references [5–7].

To further our understanding of the conditions favorable to robust pairing it would seem natural to carry out similar types of analyses of superconductivity on the border of other types of instabilities. We consider the possibility of pairing near instabilities signalled by the divergence of a particle density response function. This could include in principle structural instabilities characterized by the softening of phonons in some regions of the Brillouin zone. The induced interaction produced by these soft phonons, in contrast to conventional phonons, is non-local in space. Therefore, one could expect some similarities to the magnetic pairing problem studied in references [5–7].

A density response function may also be expected to be strongly enhanced on the border of a charge density wave (CDW) transition, a stripe instability and an $\alpha - \gamma$ or valence instability. The appropriate density response function may be expected to become large at a wavevector near the Brillouin zone boundary for a CDW, at small but finite wavevectors for stripes and at zero wavevector near the $\alpha - \gamma$ transition (at which the structure of the unit cell remains the same, but its volume changes).

We note that if the density transition happens to be strongly first order, the appropriate

density response function and hence the associated quasiparticle interaction may not be sufficiently enhanced to lead to an observable superconducting phase. This is particularly relevant to the $\alpha - \gamma$ transition commonly found in heavy fermion systems, which is similar to the liquid-gas transition in that it is first order except at the critical end point. When the latter is at a temperature well above the expected temperature scale for pairing, the enhanced density fluctuations associated with the $\alpha - \gamma$ transition are unlikely to produce superconductivity. In the temperature region near the critical end point when density fluctuations are strong, superconductivity would be suppressed by thermal fluctuations, while in the low temperature regime the density fluctuations are too weak because of the strong first order character of the density transition. This could explain the absence of superconductivity in $CeNi$ where the critical end point is around room temperature, but the existence of superconductivity in $CeCu_2Si_2$ and $CeCu_2Ge_2$ at high pressures where a corresponding critical end point is believed to exist at low temperatures or may be just suppressed.

II. MODEL

We consider quasiparticles in a simple tetragonal lattice described by a dispersion relation

$$\begin{aligned} \epsilon_{\mathbf{p}} = & -2t(\cos(p_x) + \cos(p_y) + \alpha_t \cos(p_z)) \\ & - 4t'(\cos(p_x) \cos(p_y) + \alpha_t \cos(p_x) \cos(p_z) + \alpha_t \cos(p_y) \cos(p_z)) \end{aligned} \quad (2.1)$$

with hopping matrix elements t and t' . α_t represents the electronic structure anisotropy along the z direction. $\alpha_t = 0$ corresponds to the 2D square lattice while $\alpha_t = 1$ corresponds to the 3D cubic lattice. For simplicity, we measure all lengths in units of the respective lattice spacing. In order to reduce the number of independent parameters, we take $t' = 0.45t$ and a band filling factor $n = 1.1$ as in our earlier work [5–7].

The effective interaction between quasiparticles is taken to be the induced density-density interaction and is defined in terms of a coupling constant g and a generalized density susceptibility, which is assumed to have a simple analytical form consistent with the symmetry of the lattice,

$$\chi(\mathbf{q}, \omega) = \frac{1}{N_{\mathbf{q}_0}} \sum_{\mathbf{q}_0} \frac{\chi_0 \kappa_0^2}{\kappa^2 + \Delta(\mathbf{q}) - i \frac{\omega}{\eta(\hat{q})}} \quad (2.2)$$

where κ and κ_0 are the correlation wavevectors or inverse correlation lengths in units of the lattice spacing in the basal plane, with and without strong density correlations, respectively. The function $\Delta(\mathbf{q})$, in Eq. (2.2), is defined as

$$\Delta(\mathbf{q}) = (4 + 2\alpha_d) - 2(\cos(q_x - q_{0x}) + \cos(q_y - q_{0y}) + \alpha_d \cos(q_z - q_{0z})) \quad (2.3)$$

where α_d parameterises the density anisotropy. $\alpha_d = 0$ corresponds to quasi-2D density correlations and $\alpha_d = 1$ corresponds to 3D density correlations. The sum in Eq. (2.2) is over all the symmetry related vectors \mathbf{q}_0 , with $N_{\mathbf{q}_0}$ the number of such vectors. In the following, we only explicitly write one of the vectors. It should be understood that when we say that the incipient wavevector is, for example, $\mathbf{q}_0 = [\pi/4, 0]$, it is implied that the density response function peaks at the four wavevectors $[\pm\pi/4, 0]$, $[0, \pm\pi/4]$. The parameter $\eta(\hat{q})$ in Eq. (2.2) is defined as

$$\eta(\hat{q}) = T_{DF} \hat{q}^n \quad (2.4)$$

$$\hat{q}^2 = (4 + 2\alpha_d) - 2(\cos(q_x) + \cos(q_y) + \alpha_d \cos(q_z)) \quad (2.5)$$

where T_{DF} is a characteristic density fluctuation temperature. In Eq. (2.4), the exponent $n = 1$ if the density fluctuations are such that the total density is conserved and $n = 0$ otherwise. We note that the pole of the density response function Eq. (2.2) is purely imaginary and therefore the density fluctuations we consider are overdamped. This is believed to apply on the border of CDW, stripe and valence instabilities, but not typically for lattice density fluctuations for which the poles of the density response must have a non-negligible real component. The latter would require the inclusion of an ω^2 term with real coefficient in the denominator of Eq. (2.2).

In addition to the induced density interaction, we include an on-site Coulomb repulsion I . In the large I limit, the Cooper pair state vanishes when the interacting quasiparticles are on the same site and thus conventional isotropic s-wave pairing is excluded.

We note that in the corresponding problem of magnetic pairing the effective interaction is repulsive when the two interacting quasiparticles are on the same site in the spin-singlet channel. It is, however, attractive in the spin-triplet channel, but this is irrelevant since the required spatial antisymmetry of the pair state means that the two quasiparticles have zero probability of occupying the same site simultaneously.

A complete description of the model, the Eliashberg equations for the superconducting transition temperature and their method of solution can be found in the appendix.

III. COMPARISON OF THE DENSITY AND MAGNETIC PAIRING INTERACTIONS

Our assumed form of the density response function is similar to that of the generalized magnetic susceptibility used in our previous papers. However, there is a crucial difference in that the effective magnetic interaction depends on the relative orientation of the spins of the two quasiparticles through the factor $\sigma_1 \cdot \sigma_2$. In the spin-singlet state the expectation value of $\sigma_1 \cdot \sigma_2$ gives a factor of -3. When the interaction is oscillatory in real space, this sign change leads to an interchange of attractive and repulsive regions. Since one must choose a pair state in which the quasiparticles mainly sample the attractive region of the interaction, the sign inversion implies a change in the symmetry of the Cooper pair state as illustrated in Figs. 1a and 2a for the cases of incipient ordering wavevectors $\mathbf{q}_0 = [\pi, \pi]$ and $[\pi, 0]$ in a square lattice. For the case of small \mathbf{q}_0 , where the oscillations are essentially irrelevant in our model, the density interaction is attractive in real space for both the spin-singlet and spin-triplet states, but the magnetic interaction is attractive solely for the spin-triplet state for which the expectation value of $\sigma_1 \cdot \sigma_2$ is +1.

In our model for the generalized magnetic susceptibility we have assumed that the overall magnetization is conserved and hence $\eta(\hat{q})$ vanishes as $\mathbf{q} \rightarrow 0$. This leads to greater incoherent scattering for a nearly ferromagnetic than antiferromagnetic metal, and hence to a reduction of T_c on the border of ferromagnetism. If the fluctuations of the density are

quasi-local as in some models of valence fluctuations [16], then $\eta(\hat{q})$ does not vanish at small \mathbf{q} . This corresponds to the case $n = 0$ in Eq. (2.4). If \mathbf{q}_0 is sufficiently far away from the origin in the Brillouin zone, the precise value of n is not expected to affect the calculated T_c . Since we are not going to consider the limit $\mathbf{q}_0 = 0$, for simplicity we take $n = 1$ as in the case of the magnetic interaction.

IV. RESULTS

A. Quasi 2D: $\mathbf{q}_0 = [\pi, \pi]$ and $[\pi/m, 0]$ with $m = 1, 2, 4$

The dimensionless parameters at our disposal are $g^2\chi_0/t$, T_{DF}/t , κ_0 and κ . For comparison with results of our earlier work for the case of the magnetic interaction, we take $T_{DF} = 2t/3$ and $\kappa_0^2 = 12$. In 2D, this T_{DF} corresponds to about 1000 K for a bandwidth of 1 eV, while our choice of κ_0^2 is a representative value. We note that κ_0^2/κ^2 represents the density susceptibility enhancement factor, analogous to the Stoner factor in the case of the magnetic interaction.

The results of our numerical calculations of the mean-field critical temperature T_c as a function of $g^2\chi_0/t$ and of κ^2 is shown in Fig. 1 for $\mathbf{q}_0 = [\pi, \pi]$ in which the Cooper pair state has d_{xy} symmetry. The nodal lines of this state in real space are illustrated in Fig. 1a, which also depicts the static density interaction seen by one of the quasiparticles given that the other is at the origin. For values of the dimensionless coupling parameter $g^2\chi_0/t$ corresponding to the Random Phase Approximation (of order 10), T_c is found to drop very rapidly as one goes away from the instability, i.e with increasing κ^2 .

The corresponding plots for the cases $\mathbf{q}_0 = [\pi/m, 0]$, where $m = 1, 2$ and 4 are shown in Fig. 2, 3 and 4. In contrast to the case $\mathbf{q}_0 = [\pi, \pi]$, the next-nearest-neighbor interaction for $\mathbf{q}_0 = [\pi, 0]$ is repulsive. This requires nodal lines along the diagonal, and hence the $d_{x^2-y^2}$ instead of d_{xy} symmetry. As shown in Fig. 2a, the nearest-neighbor interaction vanishes for the special case $\mathbf{q}_0 = [\pi, 0]$ and the leading attraction comes from third-nearest-neighbors.

This explains why pairing is not as robust in this case compared with the case $\mathbf{q}_0 = [\pi, \pi]$.

As seen from Figs 3a and 4a, the strength of the nearest-neighbor attraction increases as \mathbf{q}_0 gets smaller, which correlates with the increased robustness of T_c .

As \mathbf{q}_0 decreases the density interaction can also be attractive for other pairing states. In order to avoid the on-site Coulomb interaction, one could use the d_{xy} state since the next-nearest-neighbor interaction is attractive for sufficiently small \mathbf{q}_0 . But since the $d_{x^2-y^2}$ state picks the nearest-neighbor attraction, which is dominant, it is expected to be the favored state. For small \mathbf{q}_0 , the density interaction is also attractive in the spin-triplet channel for a p_x or p_y Cooper state. This state picks two out of the four nearest-neighbor attractive sites, instead of all four for the $d_{x^2-y^2}$ state. However, the p_x or p_y state also picks the attraction on all four next-nearest-neighbor sites where the $d_{x^2-y^2}$ state vanishes. It is thus not immediately obvious in that case which of the two pairing states has the highest T_c . Fig. 5 shows the Eliashberg superconducting transition temperature one obtains for the spin-triplet p_x and spin-singlet $d_{x^2-y^2}$ states as a function of the correlation wavevector κ^2 for $g^2\chi_0/t = 10$. The plot shows that the $d_{x^2-y^2}$ is the favored case and we have found this to be true for the range of values of κ^2 and $g^2\chi_0/t$ studied in this paper.

B. 3D: $\mathbf{q}_0 = [\pi, \pi, \pi]$, $\mathbf{q}_0 = [\pi/4, 0, 0]$

The results of the numerical calculations in 3D are shown in Figs 6 and 7 for $\mathbf{q}_0 = [\pi, \pi, \pi]$ in the d_{xy} Cooper state and $\mathbf{q}_0 = [\pi/4, 0, 0]$ in the $d_{x^2-y^2}$ Cooper state, respectively. The pairing for $\mathbf{q}_0 = [\pi/4, 0, 0]$ is more robust than for $\mathbf{q}_0 = [\pi, \pi, \pi]$ since the dominant attraction comes from nearest neighbor in the former case rather than next-nearest-neighbor as in the latter case. For $\mathbf{q}_0 = [\pi, \pi, \pi]$, pairing is less robust in 3D than for the corresponding quasi-2D case shown in Fig. 1 for all coupling constants. In the case $\mathbf{q}_0 = [\pi/4, 0, 0]$, pairing is more robust in quasi-2D (Fig. 4) than in the corresponding 3D case for weak to intermediate coupling. At strong coupling, however, pairing is more robust in 3D, but coupling constants $g^2\chi_0/t$ in the 20-60 range are less physically realistic.

C. Crossover from 3D to quasi-2D: Tetragonal lattice with $\mathbf{q}_0 = [\pi, \pi, \pi]$, $\mathbf{q}_0 = [\pi/4, 0, 0]$

The calculated T_c as a function of the electronic and density response anisotropy parameters α_t and α_d , respectively, are shown in Figs. 8 and 9 for representative values of the parameters κ^2 and $g^2\chi_0/t$. The results reported in sections A and B correspond to the quasi-2D case $\alpha_t = \alpha_d = 0$ and to the 3D case $\alpha_t = \alpha_d = 1$.

For $\mathbf{q}_0 = [\pi, \pi, \pi]$, shown in Fig. 8, we find that T_c increases gradually and monotonically as the system becomes more and more anisotropic in the density interaction. We also note that the effect of the electronic anisotropy is much less pronounced. In the case of an incipient ordering wavevector $\mathbf{q}_0 = [\pi/4, 0, 0]$, Fig. 9 shows that T_c is maximum for an anisotropy parameter α_d between 0 and 1, namely for an anisotropic albeit not quasi-2D in the density interaction. Also note that in the $\mathbf{q}_0 = [\pi/4, 0, 0]$ case, T_c depends more strongly on the electronic anisotropy parameter α_t than for $\mathbf{q}_0 = [\pi, \pi, \pi]$.

V. DISCUSSION

A. Role of Real Space Oscillations in the Quasiparticle Interaction

When the wavevector \mathbf{q}_0 at which the density response function is a maximum lies near the Brillouin zone boundary the quasiparticle interaction has short-range real-space oscillations. As a consequence, the robustness of the pairing depends sensitively on whether one can construct a Cooper pair state from quasiparticle states near the Fermi surface such that given one quasiparticle is located at the origin, the probability of finding the second one in regions where the interaction is repulsive is minimized. For the case $\mathbf{q}_0 = [\pi, \pi]$, this forces us to consider a Cooper state with nodes along the principal (x and y) axes (see Fig. 1a).

In the density interaction channel, the dominant attraction comes from the next-nearest-neighbor sites and is typically much weaker than the dominant nearest-neighbor attraction for spin-singlet magnetic pairing for the same wavevector $\mathbf{q}_0 = [\pi, \pi]$. This explains why for

this wavevector \mathbf{q}_0 , pairing is not as robust for the density interaction as for the magnetic interaction under otherwise similar conditions.

One might think that if there were a wavevector \mathbf{q}_0 such that the interaction is attractive at the nearest-neighbor sites, one could achieve pairing in the density channel to the same degree of robustness as in the spin-singlet magnetic channel for $\mathbf{q}_0 = [\pi, \pi]$. A potential candidate wavevector is $\mathbf{q}_0 = [\pi, 0]$ since by rotating the wavevector one would rotate the oscillation pattern in real space. However, the oscillations one obtains via Eq. (2.2) are superpositions of oscillations running along the x and y directions coming from the symmetry related components with wavevectors $[\pi, 0]$ and $[0, \pi]$. These oscillations perfectly cancel at the odd sites (see Fig. 2a), and in particular at nearest-neighbor sites. The dominant attraction arises from the third-nearest-neighbors, and thus contrary to naive expectations the case with $\mathbf{q}_0 = [\pi, 0]$ leads to even weaker pairing than with $\mathbf{q}_0 = [\pi, \pi]$. Note that for the corresponding spin-singlet magnetic pairing for $\mathbf{q}_0 = [\pi, 0]$, because of the inversion of the sign of the interaction due to the spin factor $\sigma_1 \cdot \sigma_2$, the dominant attraction would now come from the next-nearest-neighbor sites. In this case, pairing would be more robust in the magnetic than in the density channel for $\mathbf{q}_0 = [\pi, 0]$, but still not as favorable as the magnetic spin singlet channel for $\mathbf{q}_0 = [\pi, \pi]$.

The robustness of density pairing for the simple tetragonal lattice is optimized for \mathbf{q}_0 close to the Brillouin zone center since in that case the interaction at all neighboring sites is maximally attractive (see Fig. 4a). In order to avoid the on-site Coulomb repulsion, the pairing state which is the solution of the gap equation (Appendix) vanishes at the origin and its symmetry is of the form p_x, p_y, d_{xy} or $d_{x^2-y^2}$. Since the $d_{x^2-y^2}$ state has maximum amplitude at nearest-neighbor sites, it has the highest T_c .

By contrast to the case of the magnetic interaction where the most robust pairing was shown in our previous work [5] to arise for $\mathbf{q}_0 = [\pi, \pi]$, in the density channel our results indicate that the optimal case is for \mathbf{q}_0 near the Brillouin zone center. Since the symmetry of the Cooper state is the same in both cases, this would suggest that still stronger pairing should arise when the system is on the border of both a magnetic instability with \mathbf{q}_0 near

$[\pi, \pi]$ and a density instability with low \mathbf{q}_0 . In that case, the two pairing mechanisms would reinforce each other rather than compete.

This observation may be very relevant to the superconductivity in f-electron compounds such as $CeCu_2Si_2$ and $CeCu_2Ge_2$. In these systems the superconductivity extends over a region in pressure containing both an antiferromagnetic and a valence instability. What is special about these materials is that the critical end point of the latter instability lies at unusually low temperatures or is incipient, which means that density fluctuations are expected to be important in the temperature regime where superconductivity is observed. Since the two instabilities do not occur at the same pressure one would expect that near the magnetic instability the pairing would be dominated by the magnetic channel and as the pressure is increased that it would cross over to a regime dominated by the density channel.

When the two instabilities are sufficiently widely separated, one might expect to see two distinct superconducting domes, one centred near the magnetic instability and the other near the density instability. A double domed superconducting temperature-pressure phase diagram has in fact been observed in $CeCu_2Si_2$ and $CeCu_2Ge_2$ systems [13,14] and in $CeNi_2Ge_2$ [15]. Some of these experimental findings have been interpreted in terms of the effects of magnetic and valence fluctuations [16].

The overall scale of T_c is set by the characteristic temperature of magnetic and density fluctuations which tends to be below 100 K in the above f-systems. One way to increase the value of T_c is to increase these characteristic temperatures. This could be achieved by looking for analogous d-metal systems with broader electron bands. The antiferromagnetic and stripe fluctuations in the cuprates may be an example where magnetic [3] and density fluctuations [17] with high characteristic temperature scales reinforce to produce high temperature superconductivity.

B. Role of Crystalline Anisotropy

The numerical results show that the robustness of density mediated superconductivity increases gradually and monotonically as one goes from a cubic to a more anisotropic tetragonal structure for $\mathbf{q}_0 = [\pi, \pi, \pi]$ and that T_c is optimum for an anisotropic albeit not quasi-2D system for $\mathbf{q}_0 = [\pi/4, 0, 0]$. One can partly understand this result by looking at the evolution of the density interaction in real space with increasing anisotropy as illustrated qualitatively in Figs. 10 and 11 for $\mathbf{q}_0 = [\pi, \pi, \pi]$ and $\mathbf{q}_0 = [\pi/4, 0, 0]$, respectively. We see that the attraction in the basal plane gets enhanced as one goes from the cubic to a more anisotropic tetragonal lattice. This enhancement is the consequence of the increase of the phase space of soft density fluctuations as one goes from a cubic to a quasi-2D structure. Note that for $\mathbf{q}_0 = [\pi/4, 0, 0]$, the model pairing potential is not continuous at $\alpha_d = 0$ since the number of peaks of the density response goes from four (at $[\pm\pi/4, 0], [0, \pm\pi/4]$) in strictly 2D to six (at $[\pm\pi/4, 0, 0], [0, \pm\pi/4, 0], [0, 0, \pm\pi/4]$) for $\alpha_d > 0$. Other than that, our model potential varies smoothly with the tetragonal distortion, parameterised by α_d in Figs. 10 and 11, and it is clear that this effect grows gradually with increasing separation between the basal planes. In our Eliashberg calculations, mass renormalization effects, which tend to suppress T_c , also increase as one goes to a more and more anisotropic crystal structure. Our results thus depend on the interplay between the strengths of the pairing interaction and mass renormalization, and the fact that the maximum T_c in the case $\mathbf{q}_0 = [\pi/4, 0, 0]$ occurs for anisotropic but not quasi-2D systems reflects the delicate balance between these opposing effects. The above given phase space argument is similar to that used to explain the increased robustness of magnetic pairing with increasing lattice anisotropy and, hence, as anticipated in Ref. [7], carries over to other pairing mechanisms treated at the one-loop mean-field level. Another potential benefit of going to a more anisotropic crystal structure is the narrowing of the electronic band and the associated increase in the electronic density of states. Our results show that in the case of $\mathbf{q}_0 = [\pi, \pi, \pi]$ and the model parameters considered, this does not play the dominant role. However, for an incipient ordering

wavevector $\mathbf{q}_0 = [\pi/4, 0, 0]$, the increase in the electronic density of states with increased lattice anisotropy plays a more important role. This effect could also be sensitive to details of the electronic and crystal structure not considered here.

The calculations presented in this paper and in our previous work [6,7] show that, in the majority of cases considered, the lattice anisotropy increases the robustness of magnetic and density pairing in the mean-field approximation. Superconducting phase fluctuations which are not included in this approximation may be expected to suppress T_c in the 2D limit. Therefore, in practice, one would think that the most favorable case for magnetic or density pairing is that of strong, but not extreme, anisotropy where the effect of the superconducting phase fluctuations are typically weak. This is to be contrasted with the effect of order parameter fluctuations on magnetic and density transitions that can be large in metals even in 3D and more so in 2D. In the case of the density transition, even a small lattice anisotropy and the resulting increase in the order parameter fluctuations can lower the critical end point significantly. By weakening the first order transition at low temperatures, this would enhance the density fluctuations that mediate the pairing on the border of the density instability and lead to a superconducting phase.

The importance of crystalline anisotropy in enhancing the superconducting T_c on the border of antiferromagnetism has been dramatically demonstrated in going from the simple cubic system $CeIn_3$ [8] to the related tetragonal compounds $CeMIn_5$ [9] where $M = Co, Rh$ and Ir , as correctly anticipated by our earlier model calculations of magnetic pairing [5–7].

In addition to an antiferromagnetic instability at relatively low pressure, $CeIn_3$ is also thought to have a strongly first order $\alpha - \gamma$ transition at high pressures [29]. Superconductivity is only observed in a narrow range of pressure and temperature around the antiferromagnetic quantum critical point. Because of the wide separation in pressure between the magnetic and density transitions and the strongly first order nature of the latter, one would expect the observed superconductivity to be magnetically mediated. In the tetragonal compounds $CeMIn_5$, however, superconductivity is observed over a wide range of pressures.

Were an $\alpha - \gamma$ transition present in these compounds, the critical end point would be expected to be at much lower temperatures than in $CeIn_3$ due to the role of anisotropy as discussed above. This would result in stronger density fluctuations in the neighborhood of the $\alpha - \gamma$ instability. Could this be another example where antiferromagnetic and low \mathbf{q}_0 density fluctuations both contribute to the attractive pairing interaction in the $d_{x^2-y^2}$ Cooper state? This would explain the unusually wide extent of the superconducting domes observed in these materials.

It would not be surprising that such a density transition has not been reported because we expect its signature to be weak. Moreover, it is likely to be observable as a well-defined transition only over a very narrow range in pressure in the temperature-pressure phase diagram and would require very careful examination pressure scans at fixed temperatures in order to detect it [18].

VI. OUTLOOK

One can expect that the total effective interaction between particles in a strongly correlated electron system to be very complex. The interaction will clearly depend on the charge, but also more generally on the spin and current carried by the particles. The border of a density or spin or current instability is characterized by strongly enhanced order-parameter fluctuations and it is therefore plausible that the dominant interaction channel is mediated by the density, spin or current fluctuations, respectively.

In this paper we have shown how the framework developed for systems on the border of magnetism can be translated to describe systems on the border of density instabilities. A striking feature of the model we have considered is that the most robust pairing is obtained in the spin-singlet $d_{x^2-y^2}$ Cooper state on the border of both the density and spin instabilities. However, crucially the wavevector \mathbf{q}_0 at which the response function is most enhanced is different in the two cases. Density fluctuations give rise to the highest superconducting T_c for \mathbf{q}_0 near the center of the Brillouin zone while magnetic pairing is strongest for $\mathbf{q}_0 = [\pi, \pi]$.

While it is possible to construct a Cooper pair state that samples mainly the most attractive regions of the density and magnetic interaction for $\mathbf{q}_0 = [\pi, \pi]$, the attraction is weaker in the density channel because the minimum separation of the two interacting particles is larger in the d_{xy} state for the density interaction than in the $d_{x^2-y^2}$ state for the magnetic interaction (Fig. 1a). For low \mathbf{q}_0 , however, the density interaction is mostly attractive provided that the particles are not on the same site (Fig. 4a) and thus the most favored state is $d_{x^2-y^2}$ in which the two interacting particles can take advantage of the strong nearest-neighbor attraction.

It would seem that the same argument could apply to the low \mathbf{q}_0 magnetic interaction. However, in contrast to the density interaction which has the same sign in the spin-singlet and spin-triplet channels, the magnetic interaction depends on the relative spin orientation of the two interacting particles and thus has a different sign for the two cases. Magnetic pairing in the spin-singlet state is only possible if the real space interaction has sufficiently short-wavelength oscillations. Therefore, when \mathbf{q}_0 is near the center of the Brillouin zone magnetic pairing in the spin-singlet state is not possible, but is allowed in principle in the spin-triplet state for which the magnetic interaction has the opposite sign. However, magnetic pairing in this state has the disadvantage that only the exchange of spin fluctuations polarized along the direction of the interacting spins, i.e., the longitudinal fluctuations contribute to the particle interaction. For a spin rotationally invariant system, both the longitudinal and transverse spin fluctuations contribute to pairing only for a spin-singlet Cooper state. For the model considered in Refs [5–7] this effect results in much weaker pairing on the border of ferromagnetism ($\mathbf{q}_0 = 0$) than antiferromagnetism with $\mathbf{q}_0 = [\pi, \pi]$.

Another disadvantage of being on the border of ferromagnetism is that for otherwise similar conditions the suppression of T_c due to the self-interaction arising from the exchange of magnetic fluctuations is stronger than in the corresponding case on the border of antiferromagnetism. This disadvantage can be mitigated in systems with strong magnetic anisotropy in that the effect of the transverse magnetic fluctuations on the self-interaction would be suppressed while the strength of the pairing interaction arising from the longitudinal mag-

netic fluctuations need not be reduced. This may apply in systems with strong spin-orbit interactions or in the spin-polarized state close to the border of ferromagnetism.

These arguments [5,6] have stimulated a new search for evidence of superconductivity on the border of itinerant electron ferromagnetism in cases where spin anisotropy is expected to be pronounced, such as UGe_2 . This search has proved fruitful because it led to the first observation of the coexistence of superconductivity and itinerant electron ferromagnetism in UGe_2 [10] and shortly thereafter in $ZrZn_2$ [12] and $URhGe$ [11].

In the previous section and in Figs. 10 and 11 we gave simple arguments to explain how the pairing effect of the interactions are strengthened by a tetragonal distortion in our model. However, the same effects also contribute to an enhanced self-interaction which acts to suppress T_c . The relative importance of the pair-forming and pair-breaking effects of the effective interaction cannot be inferred solely from the above physical picture for the density channel and the analogous arguments given in Ref. [7] for the magnetic channel. The numerical calculations show that for most cases considered here and in Ref. [7] the pair-forming effects dominate.

A most striking manifestation of the interplay between the pair-forming and pair-breaking tendency of both the density and magnetic interactions is the breakdown of the McMillan-style expression for T_c . This was noted in Refs. [5–7] and has been interpreted in Ref. [19] in terms of the important role played by the incoherent part of the Green function which is ignored in the simplest treatments, but is included in the present and earlier work where the full momentum and frequency dependence of the self-energy is taken into account.

In this and our earlier work we deliberately avoided modelling a specific system since our main goal is to gain insights into the nature of the pairing problem on the border of a density and spin instabilities. We have focussed on understanding trends and certain general factors affecting the robustness of the pairing mechanism. Even the simplest models considered display surprising sensitivity to factors such as the nature of the instability, the wavevector \mathbf{q}_0 at which it occurs, the total spin of the Cooper pair, details of the electronic and lattice structure as well as the form of the relevant response function. Therefore, one should

exercise caution in making quantitative comparisons between the results of our calculations and experiment.

In particular, our model may not apply to situations where there is a large, local in space, contribution to the dynamical response function. This would not contribute to the pairing interaction for anisotropic Cooper states, but could greatly enhance the self-interaction effect that is pair-breaking. This could for instance greatly increase the sensitivity of T_c to lattice anisotropy as observed in $CeMIn_5$ systems and to the correlation length ($1/\kappa$) characterising the relevant response function as indirectly seen in the strong pressure dependence of T_c in, for example, $CeIn_3$. Such a local contribution to the magnetic response function has been observed in heavy fermion systems [20].

The results of the calculations would be very sensitive to the particular choice of the wavevector dependence of the response function. In cases where it falls off in \mathbf{q} faster than in our model, the response is appreciably enhanced in a smaller portion of the Brillouin zone and one would then expect the effect of the density or magnetic interaction on the thermal, transport and superconducting properties to be reduced. This could explain the surprisingly weak effects on these properties of the CDW fluctuations in systems such as $NbSe_2$ [21].

At first sight, our results seem to imply that anisotropic forms of superconductivity should be a generic property of systems on the border of density and magnetic instabilities. It may seem surprising therefore that there are still relatively few observations of this phenomenon. In addition to the sensitivity of T_c to details of the system as discussed above, in many cases the multiplicity of bands and lattice structure may be unfavorable for pairing to such an extent that quenched disorder may completely suppress superconductivity. An illustration of this latter point is the dramatic collapse of the spin-triplet superconducting T_c in Sr_2RuO_4 in the presence of Al impurity concentrations as low as 0.1% [22]. Another factor that may explain the absence of superconductivity is the common occurrence of first order rather than continuous magnetic as well as density instabilities. Our results show that in many cases one has to be close to the instability. A first order transition may make this region of the phase diagram inaccessible.

The results of the mean-field calculations presented here and in our earlier papers show that robust pairing can occur in both density and magnetic channels under suitable conditions. Therefore, it would seem that one should not favor one mechanism over another in the search for new examples of high temperature superconductivity. This conclusion may turn out to be incorrect when corrections to the one-loop mean-field calculations are taken into account. In contrast to the conventional electron-phonon pairing theory where corrections to the Eliashberg value of T_c are small, it has been argued for many years [23] that this may not be the case for other types of pairing mechanisms.

It has been shown that the mean-field approximation of the kind we have considered here qualitatively breaks down in a half-filled Hubbard model in 2D which is a Mott insulator with long-range antiferromagnetic order at absolute zero. This breakdown has been interpreted in terms of the effect of thermal magnetic fluctuations in the renormalized classical regime [24]. Thermal density fluctuations near Peirels CDW transition in 2D also lead to qualitative changes to the electronic spectrum that are not captured in the present model [25].

Recent non-perturbative calculations have shown that dynamical fluctuations even at the Gaussian level are sufficient to cause a breakdown of the present mean-field model for sufficiently small κ^2 [26]. In this and our earlier work on the magnetic interaction model, we had to solve the Eliashberg equations for the superconducting transition temperature T_c for very many choices of model parameters. Even with the best numerical algorithms, this is only practically feasible, especially in 3D, if the overall scale of the T_c 's obtained is rather high (say of the order of $0.1t$). Our choice of the characteristic density-fluctuation temperature $T_{DF} = 2t/3$ (or spin-fluctuation temperature $T_{SF} = 2t/3$ in our earlier work) was therefore dictated by such considerations. We now know [26] that for these values of T_{DF} (or T_{SF}) and the range of other model parameters considered here and in our earlier papers that vertex corrections are important. Our results are nevertheless useful if interpreted in the following way. We expect, and have checked in a number of cases [5], that the trends in T_c/T_{DF} (or T_c/T_{SF}) are weakly dependent on the absolute scale of the characteristic temperatures T_{DF} and T_{SF} . Therefore the conclusions drawn from our calculations are expected to remain

qualitatively correct for smaller values of T_{DF} or T_{SF} and hence T_c , values for which the mean-field theory of superconductivity is likely to be more accurate.

It has generally been believed that the most important factor in determining the applicability of Migdal's theorem is the form and parameters entering the relevant fluctuation spectrum. Therefore, a surprising finding was that in the range of model parameters studied in Ref. [26], the vertex corrections to the Eliashberg self-energy led to qualitatively different electron spectral functions for a coupling to magnetic and density fluctuations with identical fluctuation spectra. In those calculations, it was found that the corrections to the Eliashberg theory enhanced the magnetic interaction, but suppressed the density interaction. This effect can readily be seen at the two-loop level.

The contribution of the transverse magnetic fluctuations to the first order vertex correction is opposite in sign to that of longitudinal ones and dominates. On the other hand, in the density channel one has essentially only 'longitudinal' fluctuations, which as in the magnetic case suppress the interaction at this level of approximation. It is also known that the two fluctuation exchange processes lead to the enhancement of the spin-singlet magnetic pairing interaction [27]. While detailed calculations of T_c beyond the single-fluctuation exchange approximation have yet to be carried out, the above findings suggest that spin-singlet magnetic pairing may turn out to be more robust than density pairing under otherwise equivalent conditions.

VII. ACKNOWLEDGMENTS

We would like to thank A.V. Chubukov, P. Coleman, F.M. Grosche, S.R. Julian, P.B. Littlewood, A.J. Millis, A.P. Mackenzie, D. Pines, D.J. Scalapino, M. Sgrist and H. Yuan, for discussions on this and related topics. We acknowledge the support of the EPSRC, the Newton Trust and the Royal Society.

VIII. APPENDIX

We consider quasiparticles on a cubic or tetragonal lattice. We assume that the dominant interaction is in the density channel and postulate the following low-energy effective action for the quasiparticles:

$$S_{eff} = \sum_{\mathbf{p}, \alpha} \int_0^\beta d\tau \psi_{\mathbf{p}, \alpha}^\dagger(\tau) (\partial_\tau + \epsilon_{\mathbf{p}} - \mu) \psi_{\mathbf{p}, \alpha}(\tau) + \frac{I}{N} \sum_{\mathbf{q}} \int_0^\beta d\tau \rho_\uparrow(\mathbf{q}, \tau) \rho_\downarrow(-\mathbf{q}, \tau) - \frac{g^2}{2N} \sum_{\mathbf{q}} \int_0^\beta d\tau \int_0^\beta d\tau' \chi(\mathbf{q}, \tau - \tau') \rho(\mathbf{q}, \tau) \rho(-\mathbf{q}, \tau') \quad (8.1)$$

where N is the number of allowed wavevectors in the Brillouin zone and the carrier density $\rho_\sigma(\mathbf{q}, \tau)$ is given by

$$\rho_\sigma(\mathbf{q}, \tau) \equiv \sum_{\mathbf{p}} \psi_{\mathbf{p}+\mathbf{q}, \sigma}^\dagger(\tau) \psi_{\mathbf{p}, \sigma}(\tau) \quad (8.2)$$

and $\rho(\mathbf{q}, \tau) = \sum_\sigma \rho_\sigma(\mathbf{q}, \tau)$. The quasiparticle dispersion relation $\epsilon_{\mathbf{p}}$ is defined in Eq. (2.1), μ denotes the chemical potential, β the inverse temperature, g^2 the coupling constant and $\psi_{\mathbf{p}, \sigma}^\dagger$ and $\psi_{\mathbf{p}, \sigma}$ are Grassmann variables. We measure temperatures, frequencies and energies in the same units. Our effective density interaction consists of an induced part, the last term in Eq. (8.1), and a local on-site Coulomb repulsion, the second term in Eq. (8.1).

The retarded generalized susceptibility $\chi(\mathbf{q}, \omega)$ that defines the effective interaction, Eq. (8.1), is defined in Eq. (2.2).

The density-fluctuation propagator on the imaginary axis, $\chi(\mathbf{q}, i\nu_n)$ is related to the imaginary part of the response function $Im\chi(\mathbf{q}, \omega)$, Eq. (2.2), via the spectral representation

$$\chi(\mathbf{q}, i\nu_n) = - \int_{-\infty}^{+\infty} \frac{d\omega}{\pi} \frac{Im\chi(\mathbf{q}, \omega)}{i\nu_n - \omega} \quad (8.3)$$

To get $\chi(\mathbf{q}, i\nu_n)$ to decay as $1/\nu_n^2$ as $\nu_n \rightarrow \infty$, as it should, we introduce a cutoff ω_0 and take $Im\chi(\mathbf{q}, \omega) = 0$ for $\omega \geq \omega_0$. A natural choice for the cutoff is $\omega_0 = \eta(\hat{q})\kappa_0^2$.

The Eliashberg equations for the critical temperature T_c in the Matsubara representation reduce, for the effective action Eq. (8.1), to

$$\Sigma(\mathbf{p}, i\omega_n) = g^2 \frac{T}{N} \sum_{\Omega_n} \sum_{\mathbf{k}} \chi(\mathbf{p} - \mathbf{k}, i\omega_n - i\Omega_n) G(\mathbf{k}, i\Omega_n) \quad (8.4)$$

$$G(\mathbf{p}, i\omega_n) = \frac{1}{i\omega_n - (\epsilon_{\mathbf{p}} - \mu) - \Sigma(\mathbf{p}, i\omega_n)} \quad (8.5)$$

$$\Lambda(T)\Phi(\mathbf{p}, i\omega_n) = \frac{T}{N} \sum_{\Omega_n} \sum_{\mathbf{k}} \left(g^2 \chi(\mathbf{p} - \mathbf{k}, i\omega_n - i\Omega_n) - I \right) |G(\mathbf{k}, i\Omega_n)|^2 \Phi(\mathbf{k}, i\Omega_n)$$

$$\Lambda(T) = 1 \longrightarrow T = T_c \quad (8.6)$$

where $\Sigma(\mathbf{p}, i\omega_n)$ is the quasiparticle self-energy, $G(\mathbf{p}, i\omega_n)$ the one-particle Green's function and $\Phi(\mathbf{p}, i\omega_n)$ the anomalous self-energy. The Hartree terms coming from the on-site Coulomb repulsion and induced density interaction have been absorbed in the definition of the chemical potential, which is adjusted to give an electron density of $n = 1.1$. N is the total number of allowed wavevectors in the Brillouin Zone. Eq. (8.6) has been written for spin-singlet Cooper pairs. In the spin-triplet channel, the sign and coefficient of the term $g^2 \chi(\mathbf{p} - \mathbf{k}, i\omega_n - i\Omega_n)$ remains unchanged. The on-site Coulomb interaction I in Eq. (8.6) can be ignored since in the for spin-triplet Cooper pairs, the amplitude for the two particles to be on the same site simultaneously vanishes.

The momentum convolutions in Eqs. (8.4,8.6) are carried out with a Fast Fourier Transform algorithm on a 128×128 lattice for calculations in two dimensions and $48 \times 48 \times 48$ lattice for three dimensional calculations. The frequency sums in both the self-energy and linearized gap equations are treated with the renormalization group technique of Pao and Bickers [28]. We have kept between 8 and 16 Matsubara frequencies at each stage of the renormalization procedure, starting with an initial temperature $T_0 = 0.4t$ in two dimensions and $T_0 = 0.6t$ in three dimensions and cutoff $\Omega_c \approx 30t$. The renormalization group acceleration technique restricts one to a discrete set of temperatures $T_0 > T_1 > T_2 \dots$. The critical temperature at which $\Lambda(T) = 1$ in Eq. (8.6) is determined by linear interpolation.

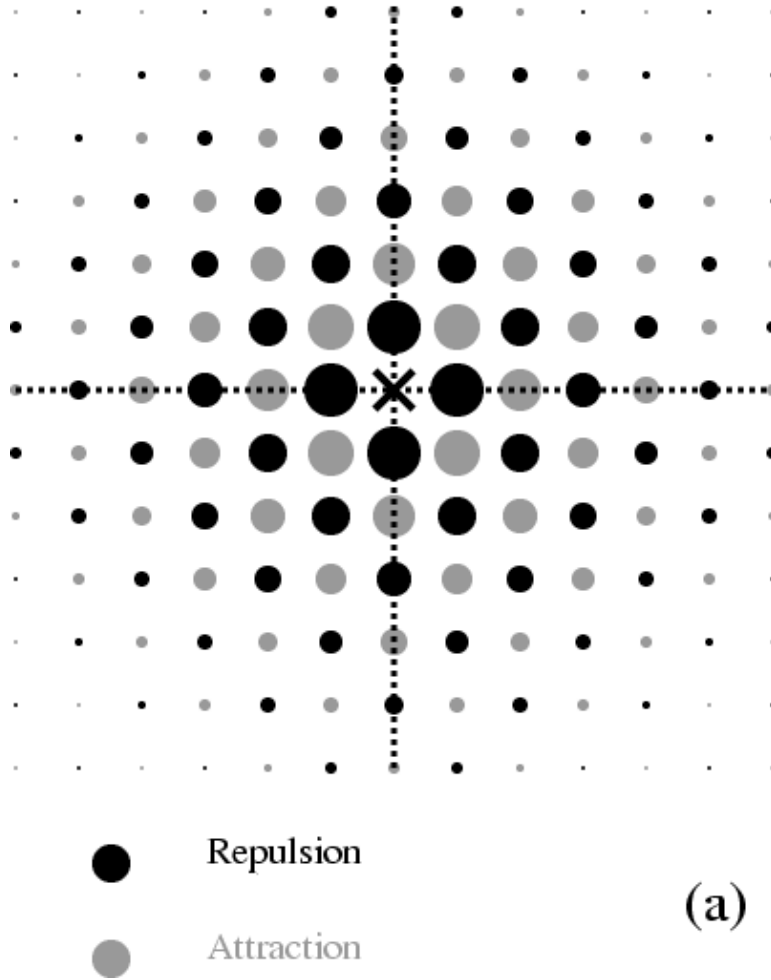
REFERENCES

- [1] J. Bardeen, L.N. Cooper and J.R. Schrieffer, Phys. Rev. **108**, 1175 (1957).
- [2] W. Kohn and J.M. Luttinger, Phys. Rev. Lett. **15**, 524 (1965).
- [3] T.Moriya, Y. Takahashi and K. Ueda, J. Phys. Soc. Jpn. **52**, 2905 (1990). P. Monthoux, A.V. Balatsky and D. Pines, Phys. Rev. Lett. **67**, 3448 (1991).
- [4] E.R. Dobbs, "Helium Three", Oxford University Press (2001).
- [5] P. Monthoux and G.G. Lonzarich, Phys. Rev. B **59**, 14598 (1999).
- [6] P. Monthoux and G.G. Lonzarich, Phys. Rev. B **63**, 054529 (2001).
- [7] P. Monthoux and G.G. Lonzarich, Phys. Rev. B **66**, 224504 (2002).
- [8] I. R. Walker, F.M. Grosche, D. M. Freye, and G.G. Lonzarich, Physica C **282**, 303 (1997).
- [9] H. Hegger, C. Petrovic, E.G. Moshopoulou, M.F. Hundley, J.L. Sarrao, Z. Fisk, J.D. Thompson Phys. Rev. Lett. **84**, 4986 (2000).
- [10] S.S. Saxena, P. Argawal, K. Ahilan, F.M. Grosche, R.K.W. Haselwimmer, M.J. Steiner, E. Pugh, I.R. Walker, S.R. Julian, P. Monthoux, G.G. Lonzarich, A. Huxley, I. Sheikin, D. Braithwaite, J. Flouquet, Nature **406**, 587 (2000).
- [11] D. Aoki, A. Huxley, E. Ressouche, D. Braithwaite, J. Flouquet, J.P. Brison, E. Lhotel, C. Paulsen, Nature **413**, 613 (2001).
- [12] C. Pfleiderer C, M. Uhlarz, S.M. Hayden, R. Vollmer, H. von Lohneysen, N.R. Bernhoeft, G.G. Lonzarich, Nature **412**, 58 (2001).
- [13] A.T. Holmes, D. Jaccard, and K. Miyake, cond-mat/0306054.
- [14] H.Q. Yuan et al., unpublished.
- [15] F.M. Grosche, P. Agarwal, S.R. Julian, N.J. Wilson, R.K.W. Haselwimmer, S.J.S Lister,

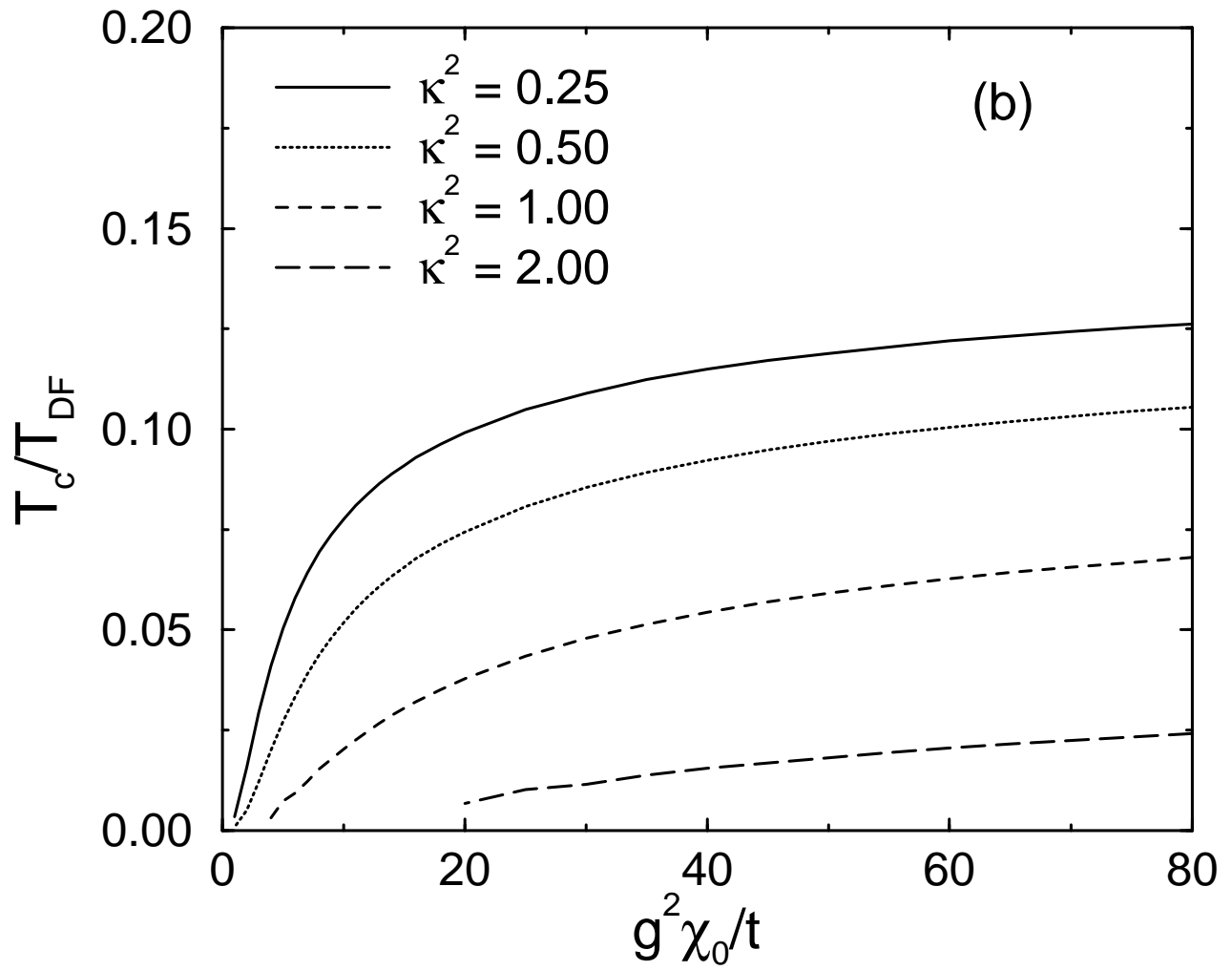
- N.D. Mathur, F.V. Carter, S.S. Saxena, G.G. Lonzarich, *J Phys-Condens. Mat.* **12**, L533 (2000).
- [16] Y. Onishi and K. Miyake, *J. Phys. Soc. Jpn.* **69**, 3955 (2000).
- [17] S. Caprara, M. Sulpizi, A. Bianconi, C. DiCastro, and M. Grilli, *Phys. Rev. B* **59**, 14980 (1999). L. Benfatto, S. Caprara, and C. DiCastro, *Eur. Phys. J. B* **17**, 95 (2000).
- [18] A. Onodera, S. Tsuduki, Y. Ohishi, T. Watanuki, K. Ishida, Y. Kitaoka, and Y. Onuki, *Solid State Commun.* **123**, 113 (2002).
- [19] A. Abanov, A.V. Chubukov, and A.M. Finkel'stein, *Europhys. Lett.* **54**, 488 (2001).
- [20] J.L. Jacoud, L.P. Regnault, J. Rossat-Mignod, C. Vettier, P. Lejay, and J. Flouquet, *J. Magn. Magn. Mater.* **108**, 131 (1992).
- [21] C. Berthier, P. Molinié, and D. Jérôme, *Solid State Commun.* **18**, 1393 (1976).
- [22] A. P. Mackenzie, R. K. W. Haselwimmer, A. W. Tyler, G. G. Lonzarich, Y. Mori, S. Nishizaki, and Y. Maeno *Phys. Rev. Lett.* **80**, 161 (1998).
- [23] J.A. Hertz, K. Levin, and M.T. Béal-Monod, *Solid State Commun.* **18**, 803 (1976).
- [24] Y.M. Vilks and A.-M. S. Tremblay, *Europhysics Lett.* **33**, 159 (1996). Y.M. Vilks and A.-M. S. Tremblay, *J. Phys. I, France* **7**, 1309 (1997). S. Moukouri, S. Allen, F. Lemay, B. Kyung, D. Poulin. Y. M. Vilks and A.-M. S. Tremblay, *Phys. Rev. B* **61**, 7887 (2000).
- [25] P. Monthoux and D.J. Scalapino, *Phys. Rev. B* **65**, 235104 (2002).
- [26] P. Monthoux, *Phys. Rev. B* **68**, 064408 (2003).
- [27] P. Monthoux, *Phys. Rev. B* **55**, 15261 (1997).
- [28] C.-H. Pao and N.E. Bickers, *Phys. Rev. B* **49**, 1586 (1994).
- [29] G. Oomi, M. Tabata and J. Sakurai *J. Magn. Magn. Mater.* **54-7**, 431 (1986).

FIGURES

Pairing Potential: Density Fluctuations $q_b = [\pi, \pi]$



Quasi 2D ; $q_0 = [\pi, \pi]$



Quasi 2D ; $\mathbf{q}_0 = [\pi, \pi]$

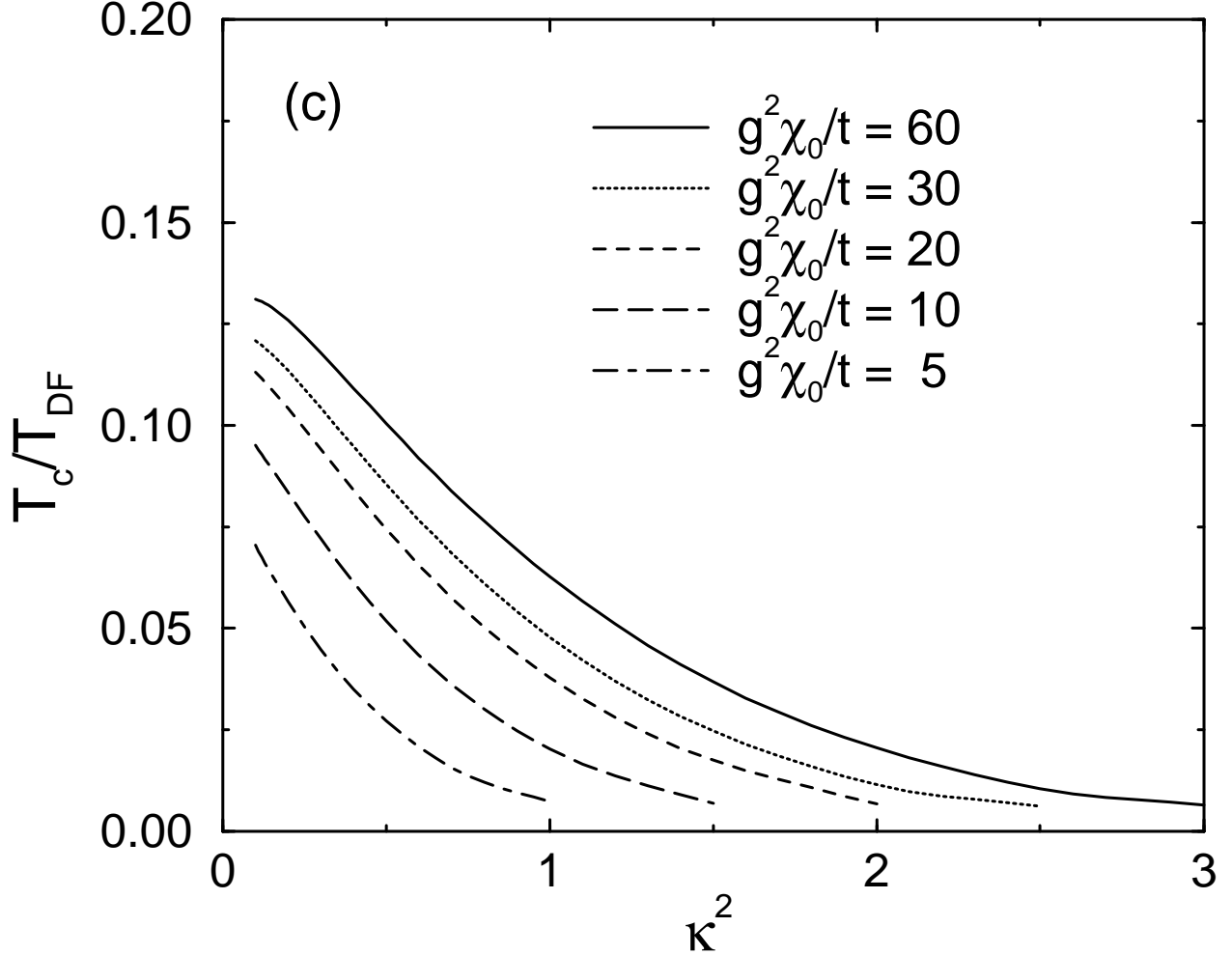
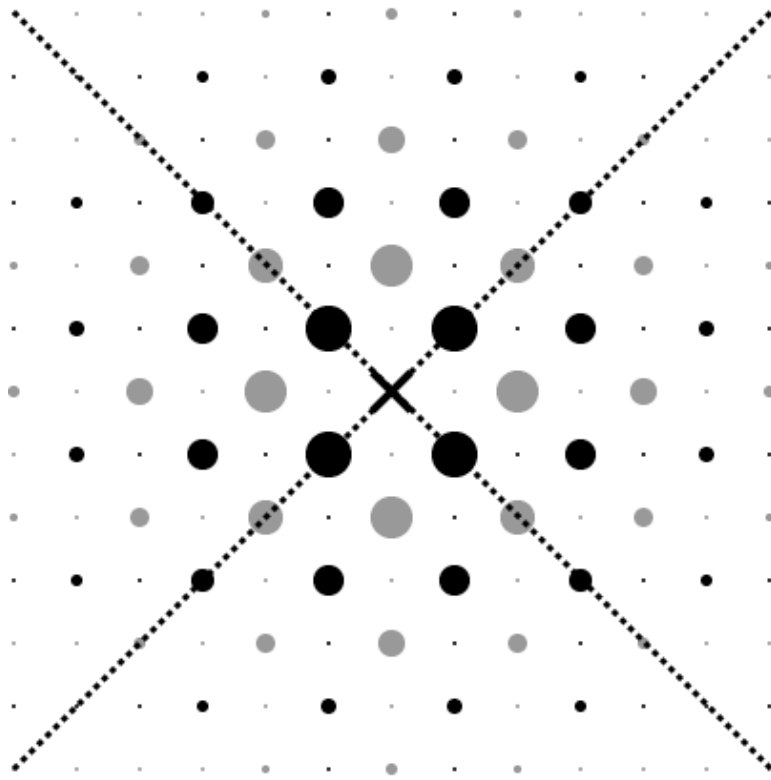


FIG. 1. (a) Static pairing potential seen by a quasiparticle in a square lattice given that the other quasiparticle is at the origin (marked by a cross) for an incipient ordering wavevector $\mathbf{q}_0 = [\pi, \pi]$. The sites are colored black if the interaction is repulsive and light gray if it is attractive. The size of the circles represents, on a logarithmic scale, the absolute value of the static pairing potential. The dashed line indicates the nodal lines of the d_{xy} Cooper state. (b) and (c) show the Eliashberg T_c/T_{DF} for a quasi two-dimensional system as a function of the coupling constant $g^2\chi_0/t$ (b) and correlation wavevector κ^2 (c) for the choice $T_{DF} = 2t/3$ and $\kappa_0^2 = 12$.

Pairing Potential: Density Fluctuations $q_b = [\pi, 0]$

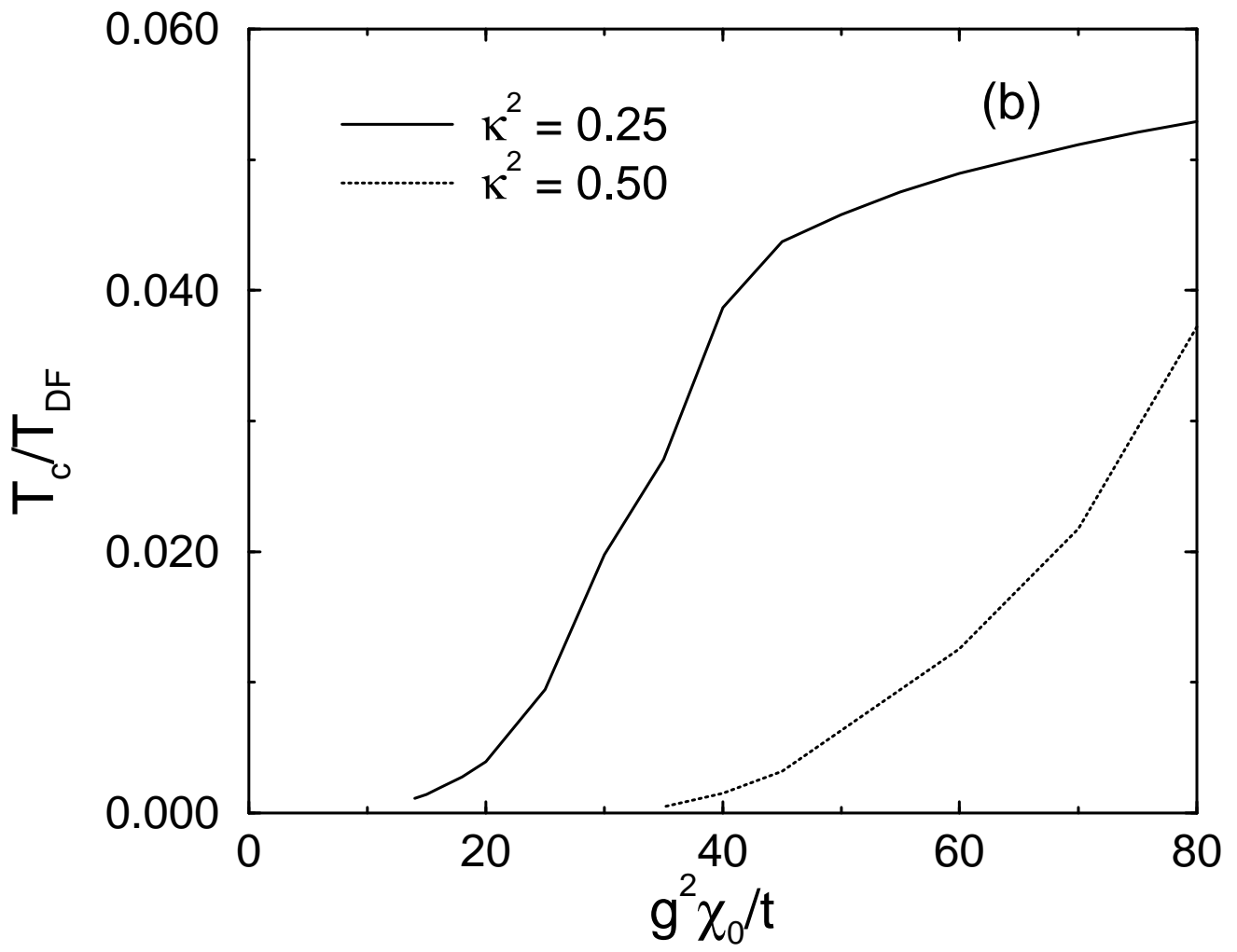


● Repulsion

● Attraction

(a)

Quasi 2D ; $q_0 = [\pi, 0]$



Quasi 2D ; $\mathbf{q}_0 = [\pi, 0]$

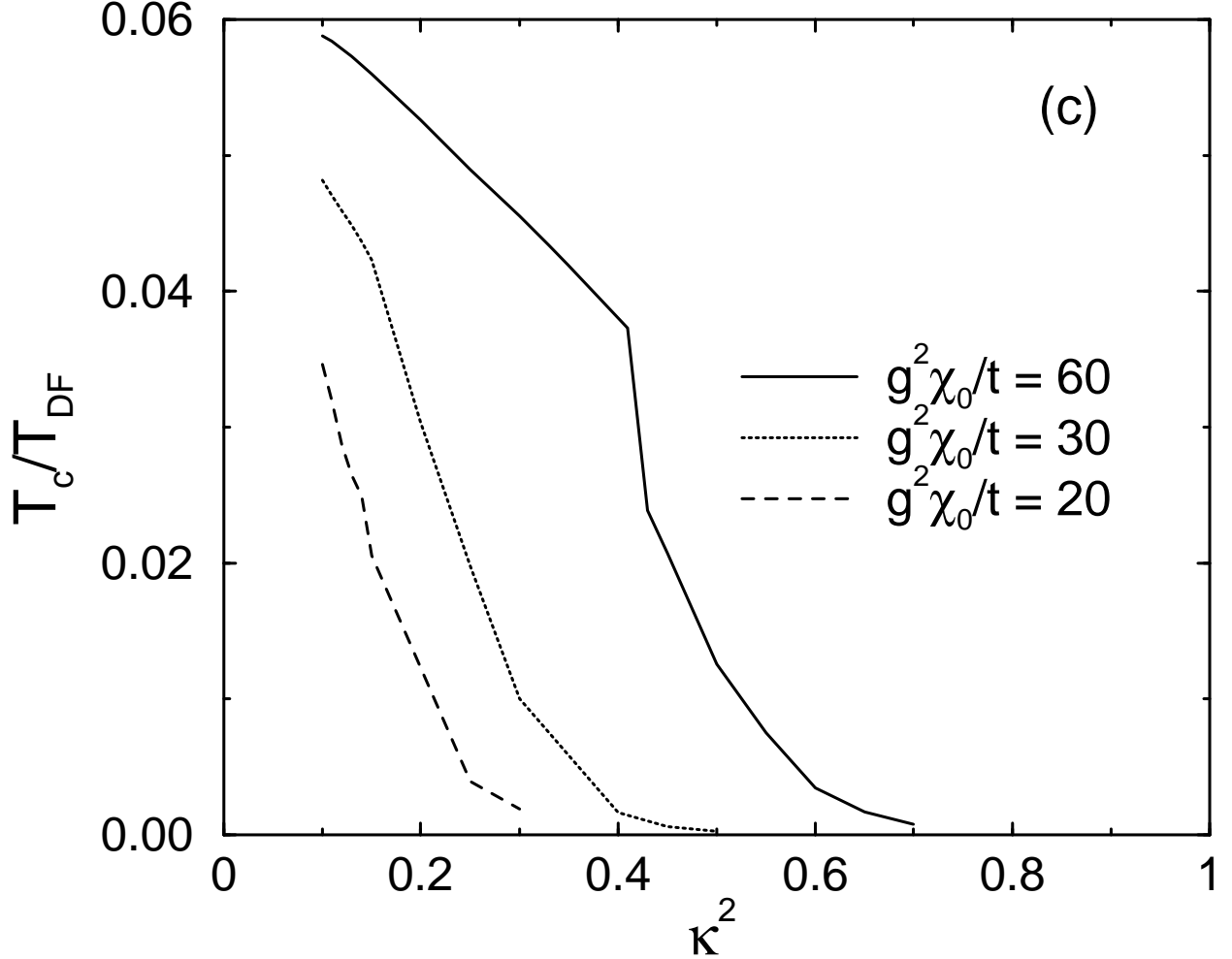
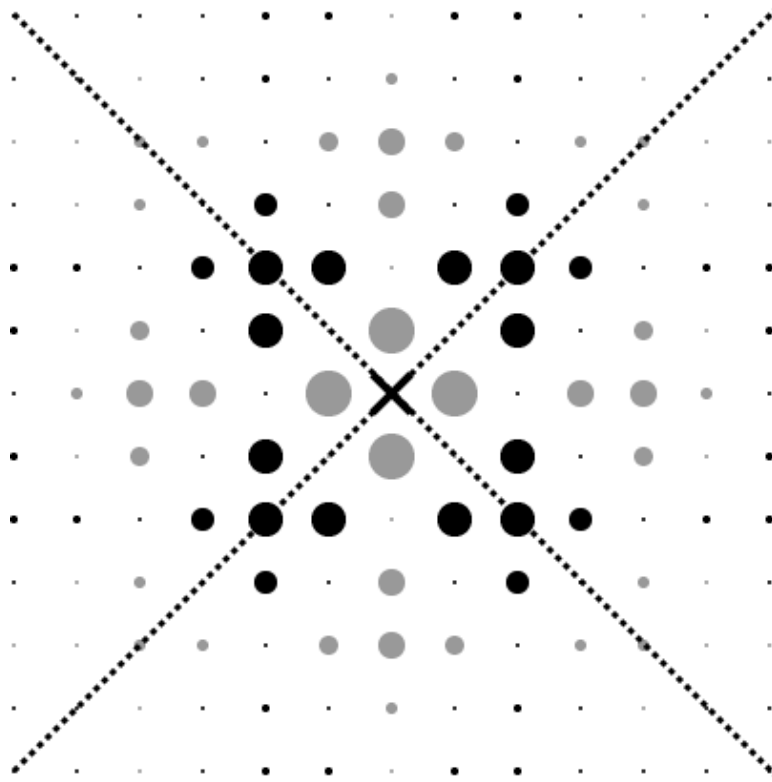


FIG. 2. (a) Static pairing potential seen by a quasiparticle in a square lattice given that the other quasiparticle is at the origin (marked by a cross) for an incipient ordering wavevector $\mathbf{q}_0 = [\pi, 0]$. The sites are colored black if the interaction is repulsive and light gray if it is attractive. The size of the circles represents, on a logarithmic scale, the absolute value of the static pairing potential. The dashed line indicates the nodal lines of the $d_{x^2-y^2}$ Cooper state. (b) and (c) show the Eliashberg T_c/T_{DF} for a quasi two-dimensional system as a function of the coupling constant $g^2\chi_0/t$ (b) and correlation wavevector κ^2 (c) for the choice $T_{DF} = 2t/3$ and $\kappa_0^2 = 12$.

Pairing Potential: Density Fluctuations $q_b = [\pi/2, 0]$

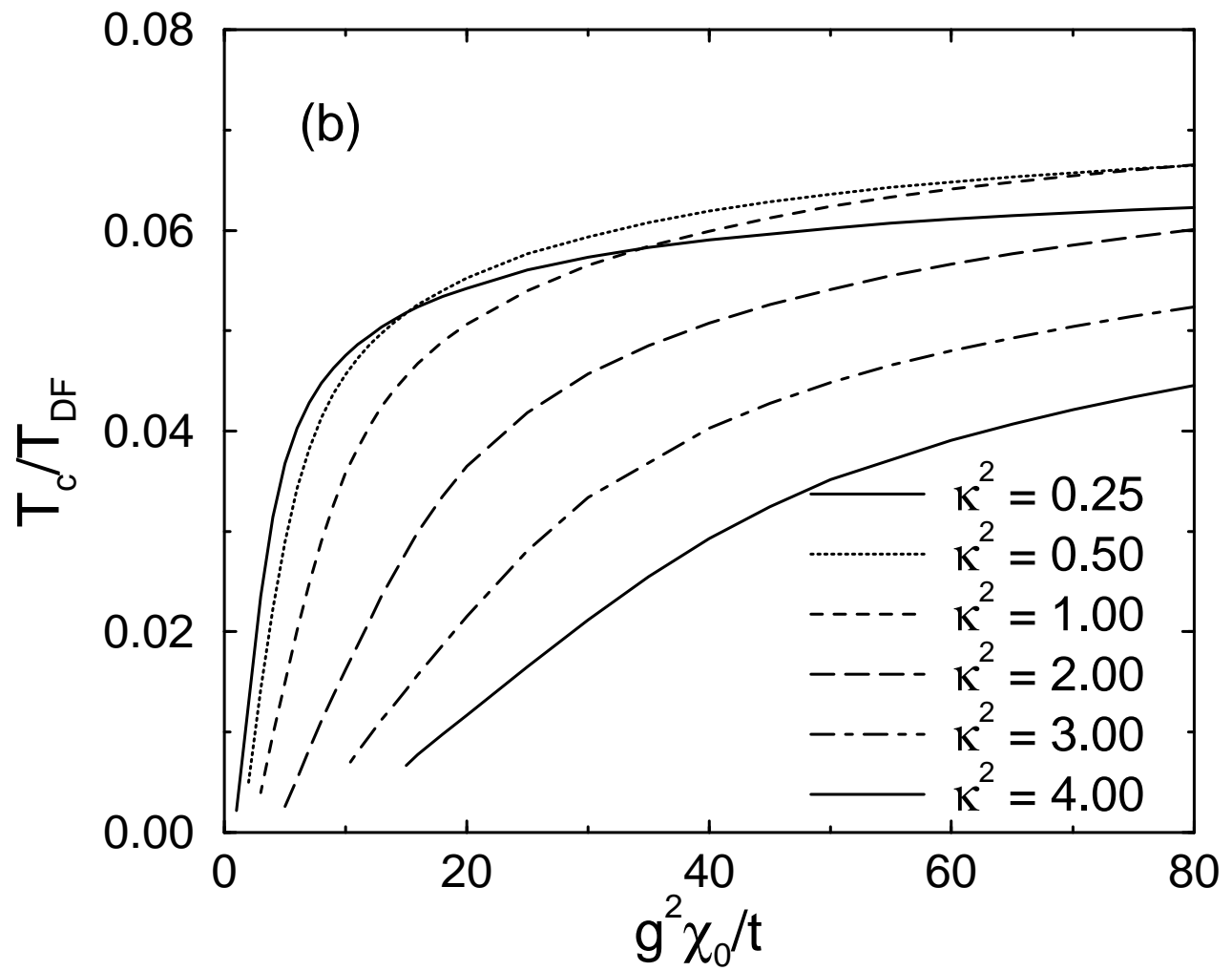


● Repulsion

● Attraction

(a)

Quasi 2D ; $q_0 = [\pi/2, 0]$



Quasi 2D ; $\mathbf{q}_0 = [\pi/2, 0]$

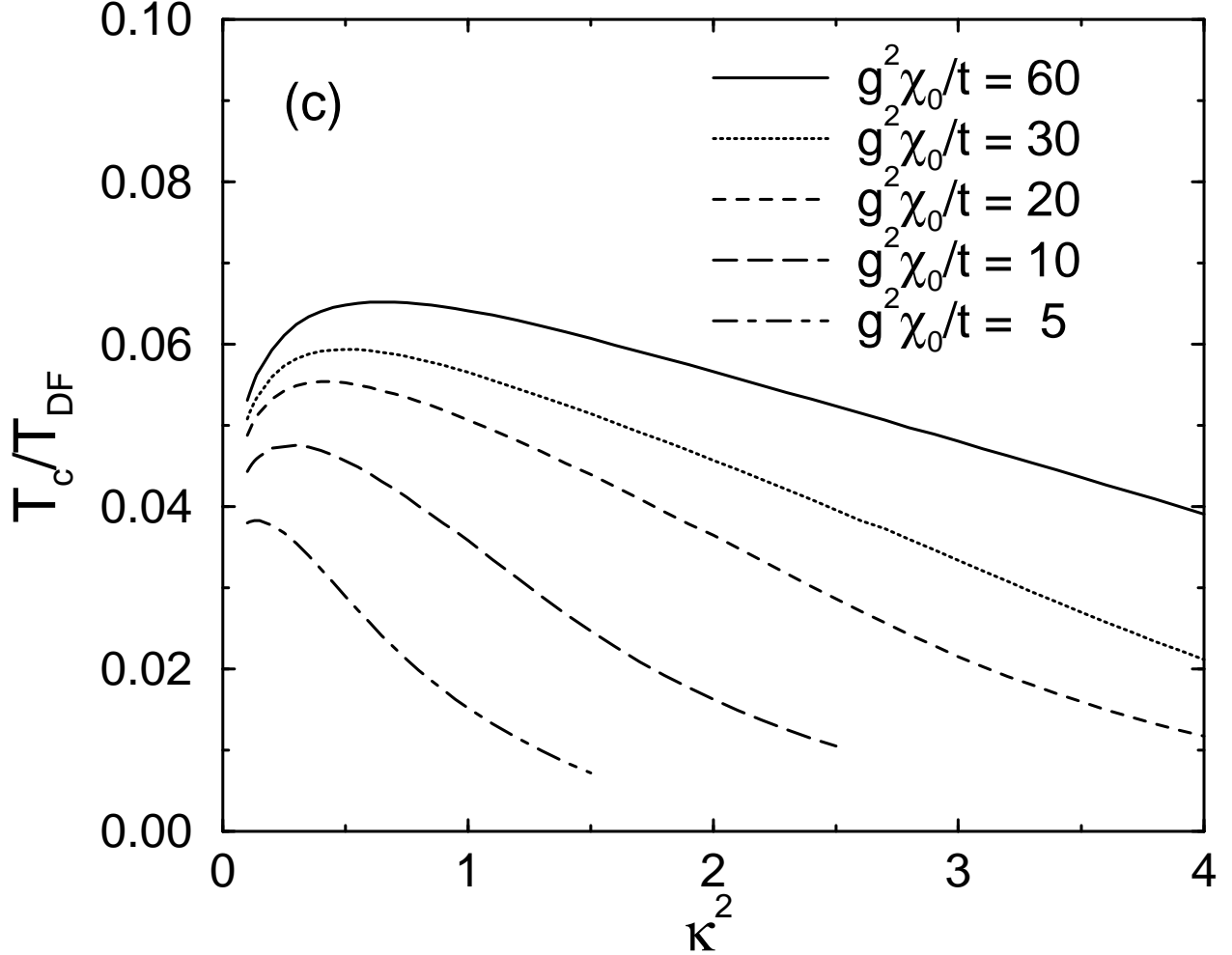
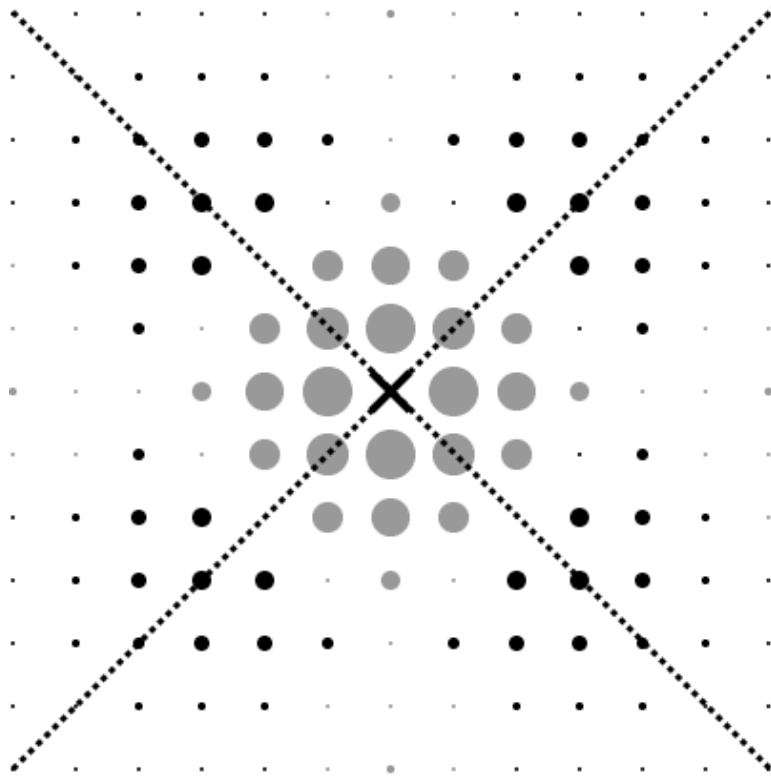


FIG. 3. (a) Static pairing potential seen by a quasiparticle in a square lattice given that the other quasiparticle is at the origin (marked by a cross) for an incipient ordering wavevector $\mathbf{q}_0 = [\pi/2, 0]$. The sites are colored black if the interaction is repulsive and light gray if it is attractive. The size of the circles represents, on a logarithmic scale, the absolute value of the static pairing potential. The dashed line indicates the nodal lines of the $d_{x^2-y^2}$ Cooper state. (b) and (c) show the Eliashberg T_c/T_{DF} for a quasi two-dimensional system as a function of the coupling constant $g^2\chi_0/t$ (b) and correlation wavevector κ^2 (c) for the choice $T_{DF} = 2t/3$ and $\kappa_0^2 = 12$.

Pairing Potential: Density Fluctuations $q_b = [\pi/4, 0]$

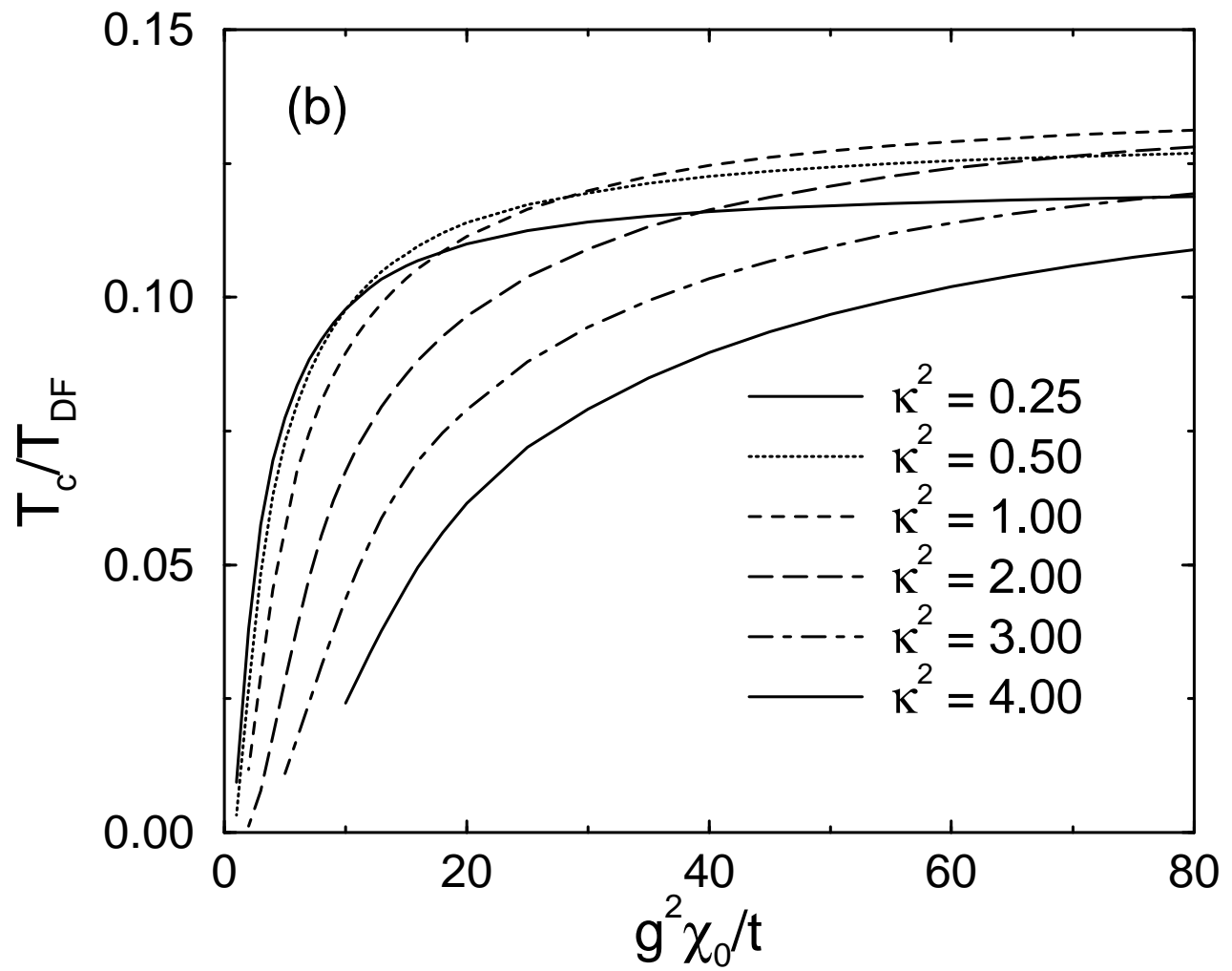


● Repulsion

● Attraction

(a)

Quasi 2D ; $q_0 = [\pi/4, 0]$



Quasi 2D ; $\mathbf{q}_0 = [\pi/4, 0]$

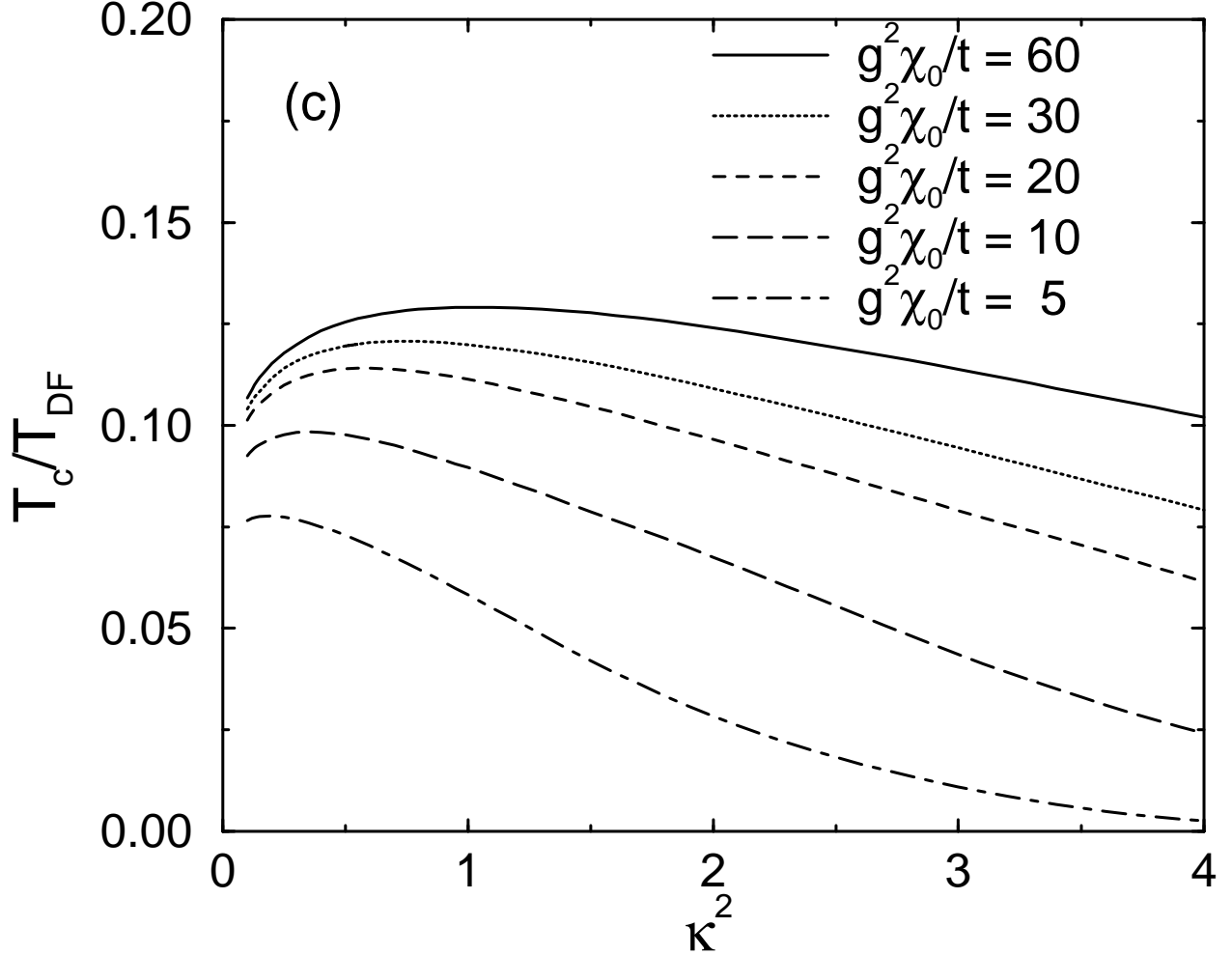


FIG. 4. (a) Static pairing potential seen by a quasiparticle in a square lattice given that the other quasiparticle is at the origin (marked by a cross) for an incipient ordering wavevector $\mathbf{q}_0 = [\pi/4, 0]$. The sites are colored black if the interaction is repulsive and light gray if it is attractive. The size of the circles represents, on a logarithmic scale, the absolute value of the static pairing potential. The dashed line indicates the nodal lines of the $d_{x^2-y^2}$ Cooper state. (b) and (c) show the Eliashberg T_c/T_{DF} for a quasi two-dimensional system as a function of the coupling constant $g^2\chi_0/t$ (b) and correlation wavevector κ^2 (c) for the choice $T_{DF} = 2t/3$ and $\kappa_0^2 = 12$.

Quasi 2D ; $\mathbf{q}_0 = [\pi/4, 0]$; $g^2 \chi_0/t = 10$

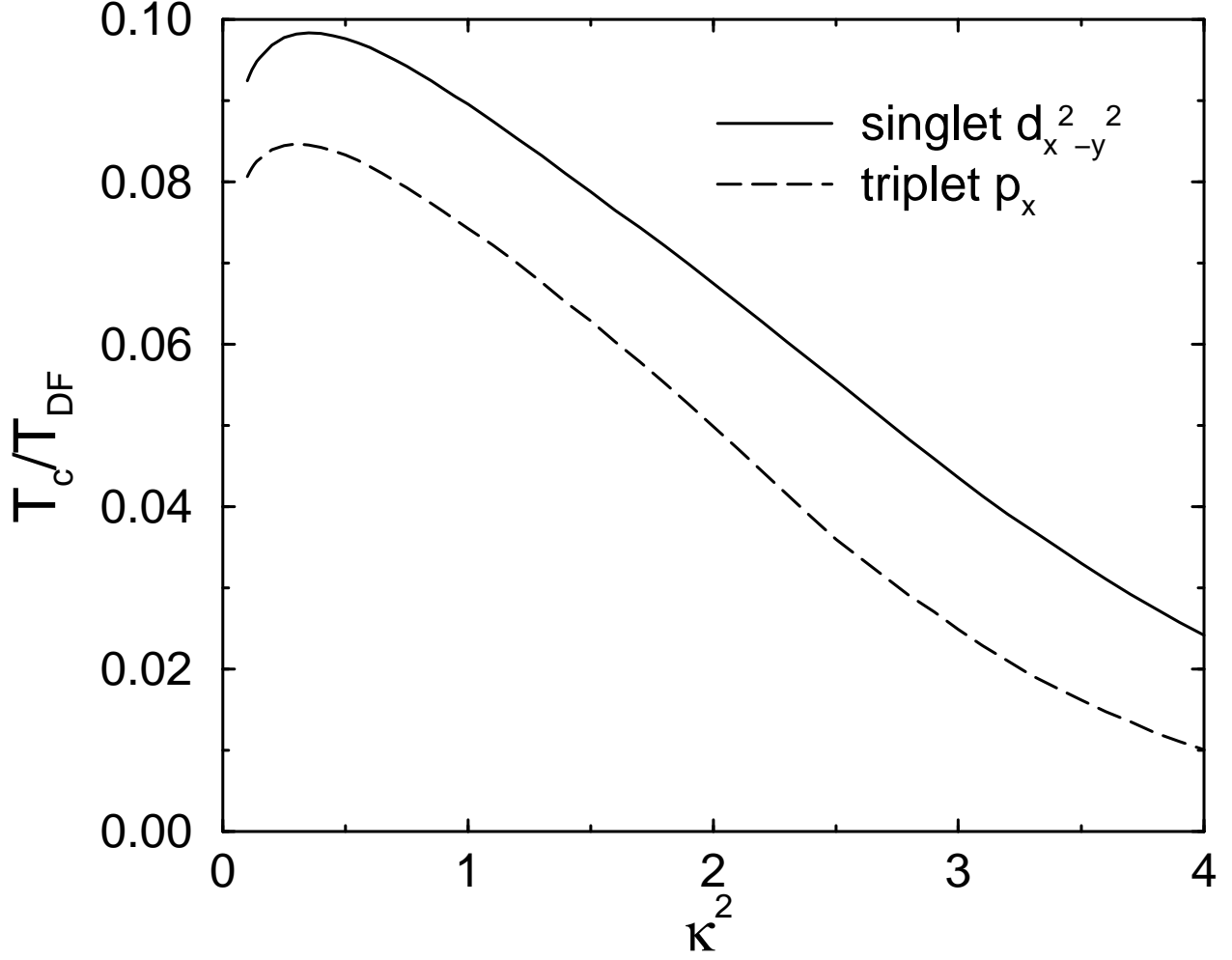
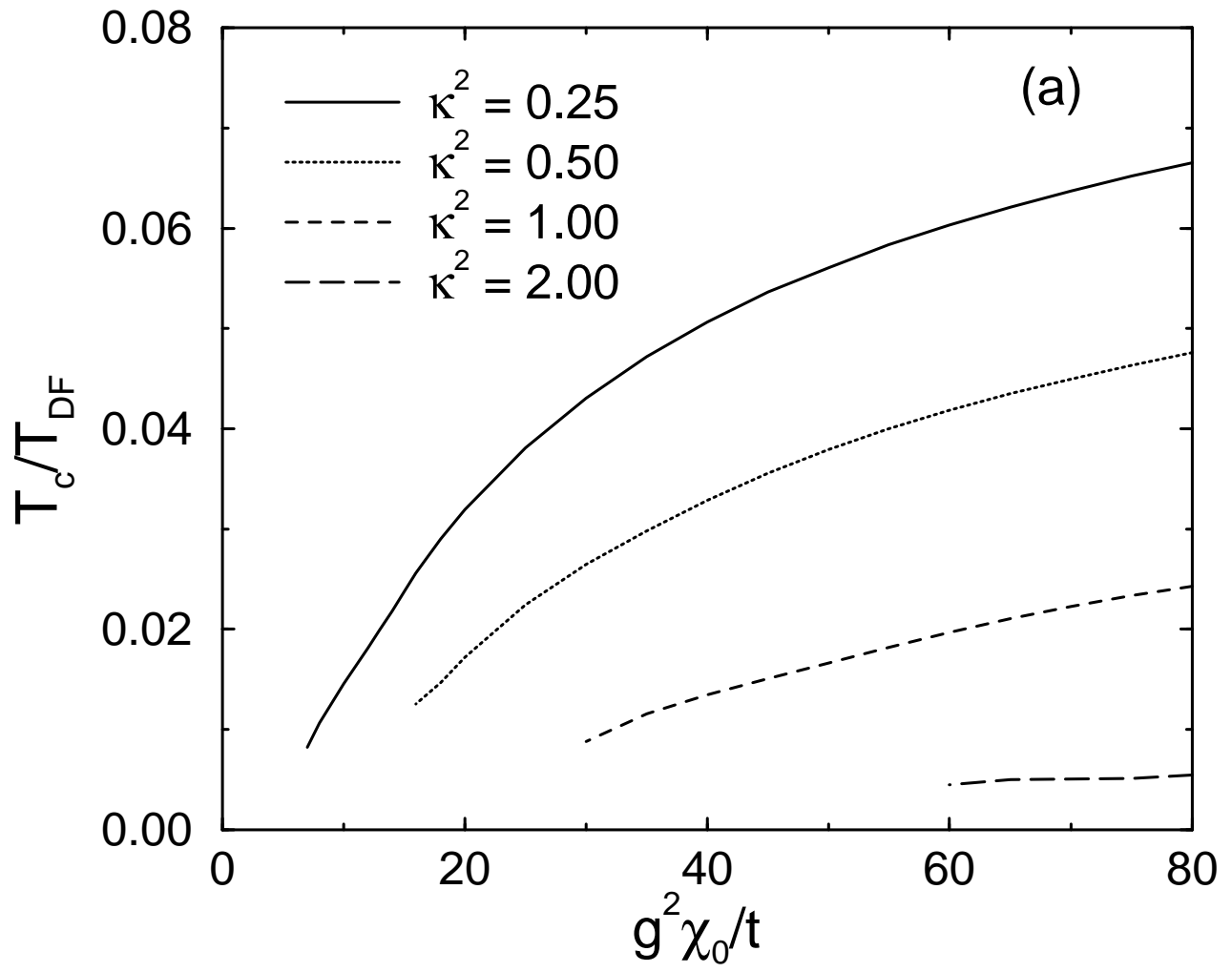


FIG. 5. Comparison of the Eliashberg T_c/T_{DF} for a quasi two-dimensional system with incipient ordering wavevector $\mathbf{q}_0 = [\pi/4, 0]$ in the spin-singlet $d_{x^2-y^2}$ versus spin-triplet p_x Cooper state. The model parameters used in the calculations are $g^2 \chi_0/t = 10$, $T_{DF} = 2t/3$ and $\kappa_0^2 = 12$.

3D ; $q_0 = [\pi, \pi, \pi]$



3D ; $\mathbf{q}_0 = [\pi, \pi, \pi]$

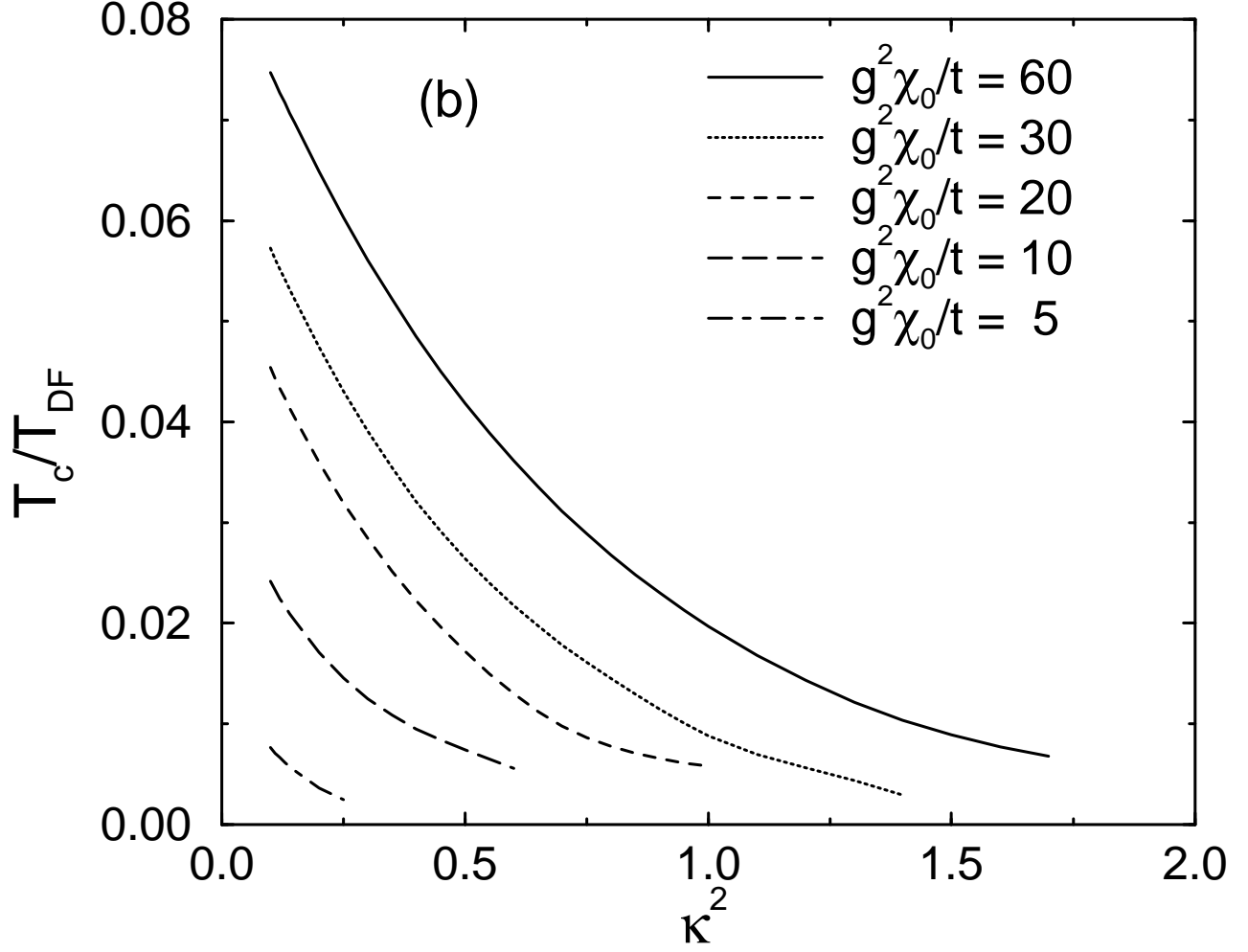
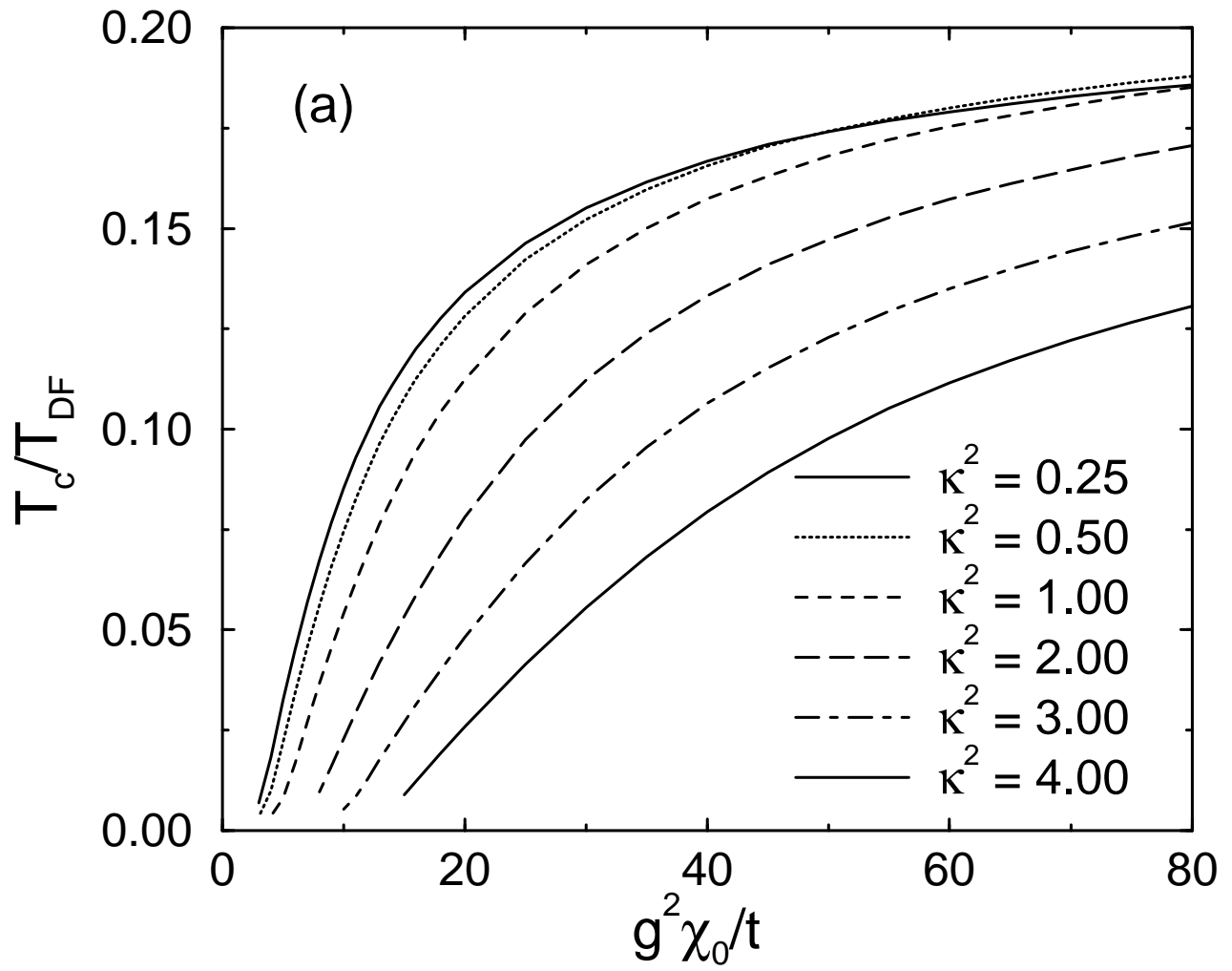


FIG. 6. (a) and (b) show the spin-singlet d_{xy} Eliashberg T_c/T_{DF} for a three-dimensional system with incipient ordering wavevector $\mathbf{q}_0 = [\pi, \pi, \pi]$ in as a function of the coupling constant $g^2\chi_0/t$ (a) and correlation wavevector κ^2 (b) for the choice $T_{DF} = 2t/3$ and $\kappa_0^2 = 12$.

3D ; $q_0 = [\pi, 4, 0, 0]$



3D ; $\mathbf{q}_0 = [\pi/4, 0, 0]$

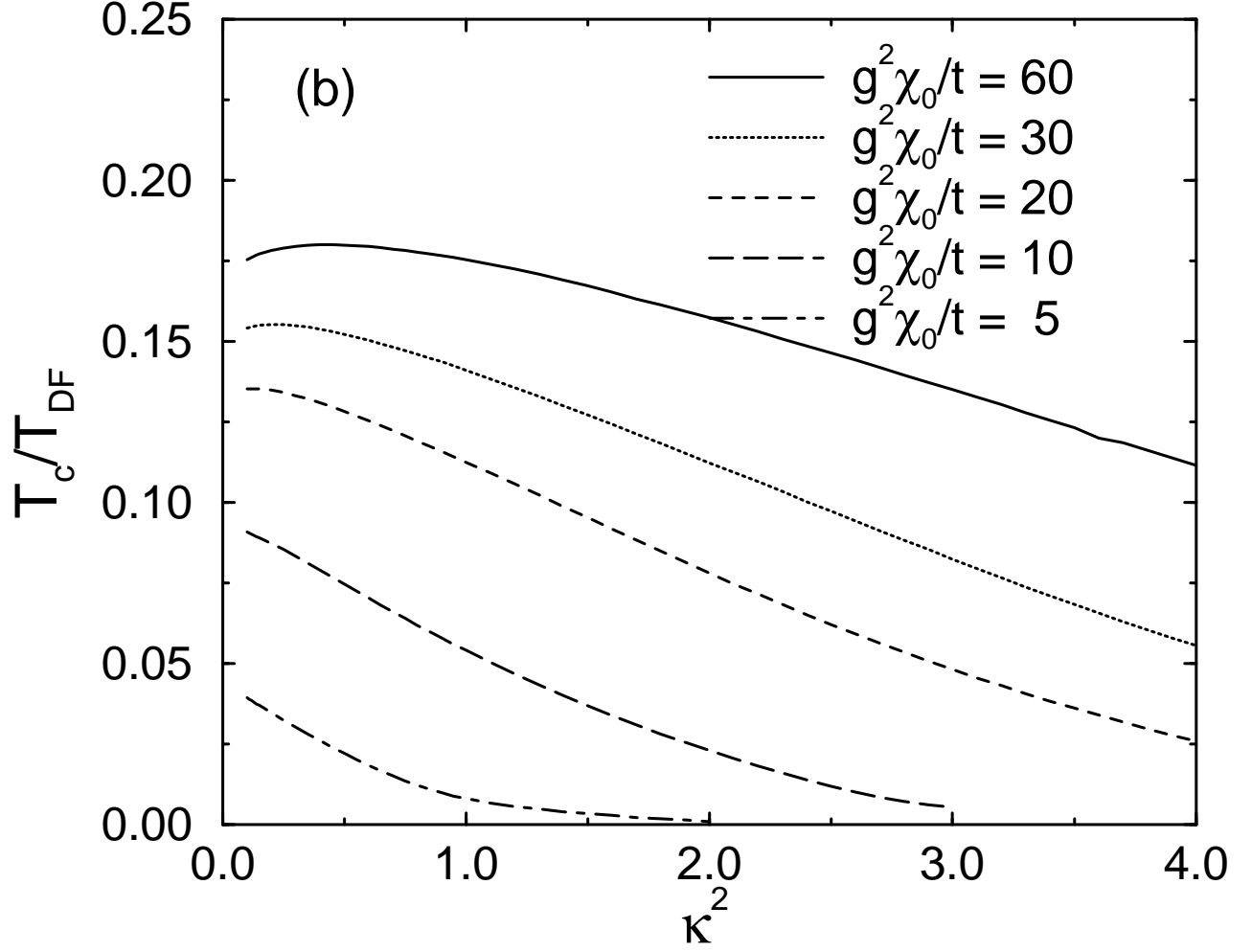


FIG. 7. (a) and (b) show the spin-singlet $d_{x^2-y^2}$ Eliashberg T_c/T_{DF} for a three-dimensional system with incipient ordering wavevector $\mathbf{q}_0 = [\pi/4, 0, 0]$ in as a function of the coupling constant $g^2\chi_0/t$ (a) and correlation wavevector κ^2 (b) for the choice $T_{DF} = 2t/3$ and $\kappa_0^2 = 12$.

$$\mathbf{q}_0 = [\pi, \pi, \pi] \quad ; \quad \kappa^2 = 0.25 \quad ; \quad g^2 \chi_0 / t = 10$$

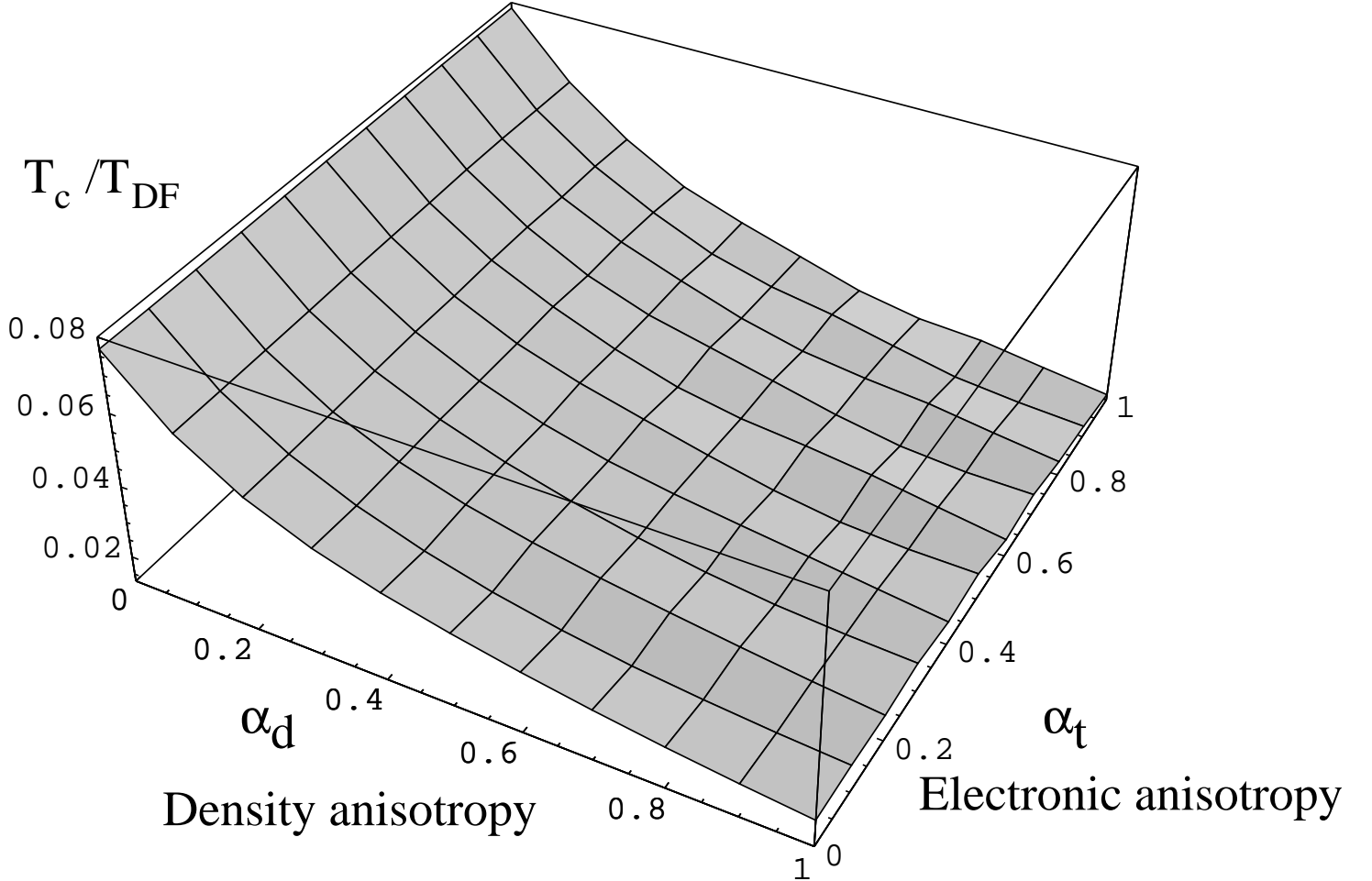


FIG. 8. Spin-singlet d_{xy} Eliashberg T_c/T_{DF} as a function of the density and electronic anisotropy parameters α_d and α_t respectively. $\alpha_d = \alpha_t = 0$ corresponds to the 2D limit while $\alpha_d = \alpha_t = 1$ corresponds to an isotropic 3D system. The incipient ordering wavevector is $\mathbf{q}_0 = [\pi, \pi, \pi]$, and the other model parameters are $\kappa^2 = 0.25$, $g^2 \chi_0 / t = 10$, $T_{DF} = 2t/3$ and $\kappa_0^2 = 12$.

$$\mathbf{q}_0 = [\pi/4, 0, 0]; \quad \kappa^2 = 0.25; \quad g^2 \chi_0 / t = 10$$

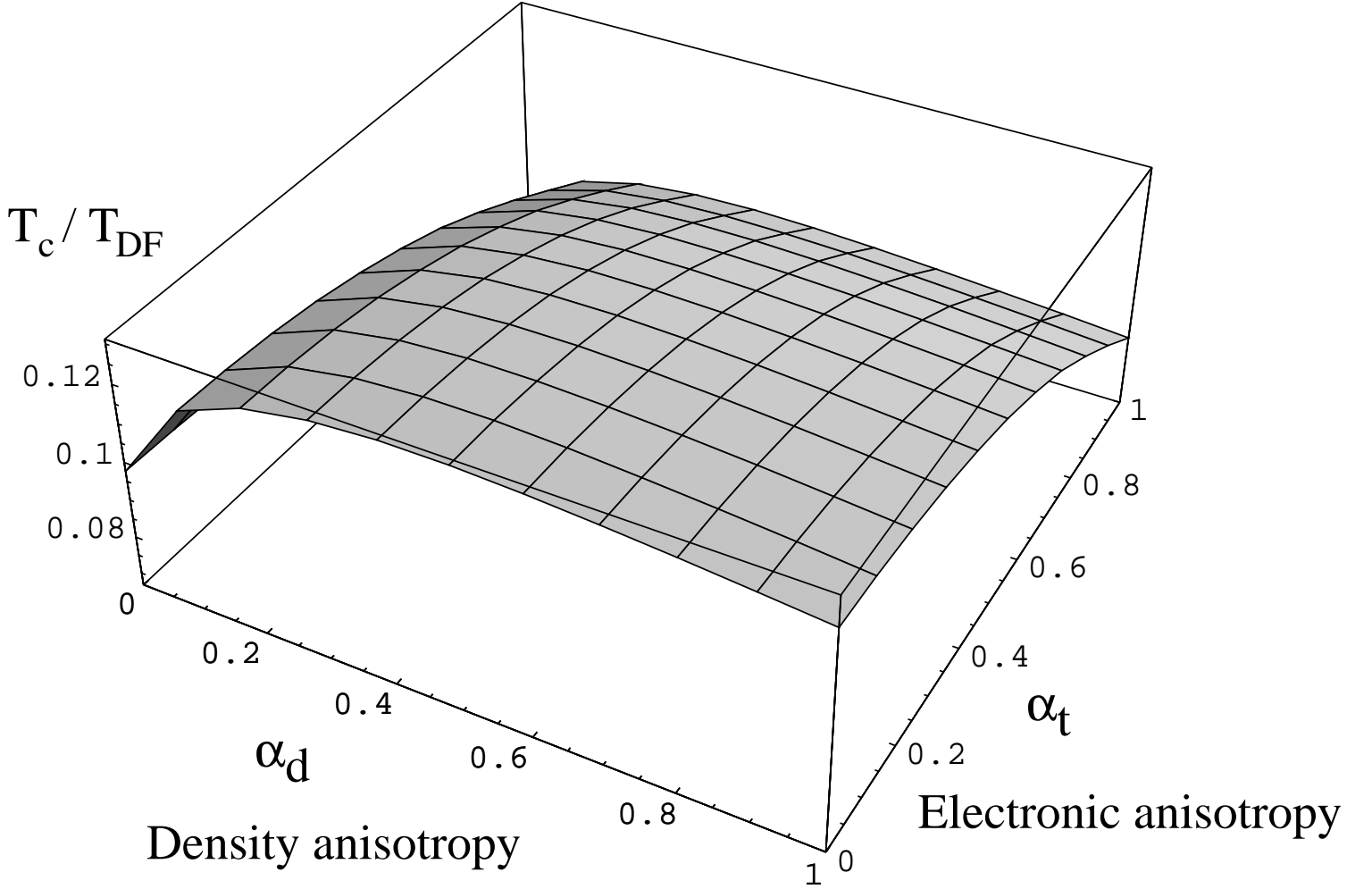


FIG. 9. Spin-singlet $d_{x^2-y^2}$ Eliashberg T_c/T_{DF} as a function of the density and electronic anisotropy parameters α_d and α_t respectively. $\alpha_d = \alpha_t = 0$ corresponds to the 2D limit while $\alpha_d = \alpha_t = 1$ corresponds to an isotropic 3D system. The incipient ordering wavevector is $\mathbf{q}_0 = [\pi/4, 0, 0]$, and the other model parameters are $\kappa^2 = 0.25$, $g^2 \chi_0 / t = 10$, $T_{DF} = 2t/3$ and $\kappa_0^2 = 12$.

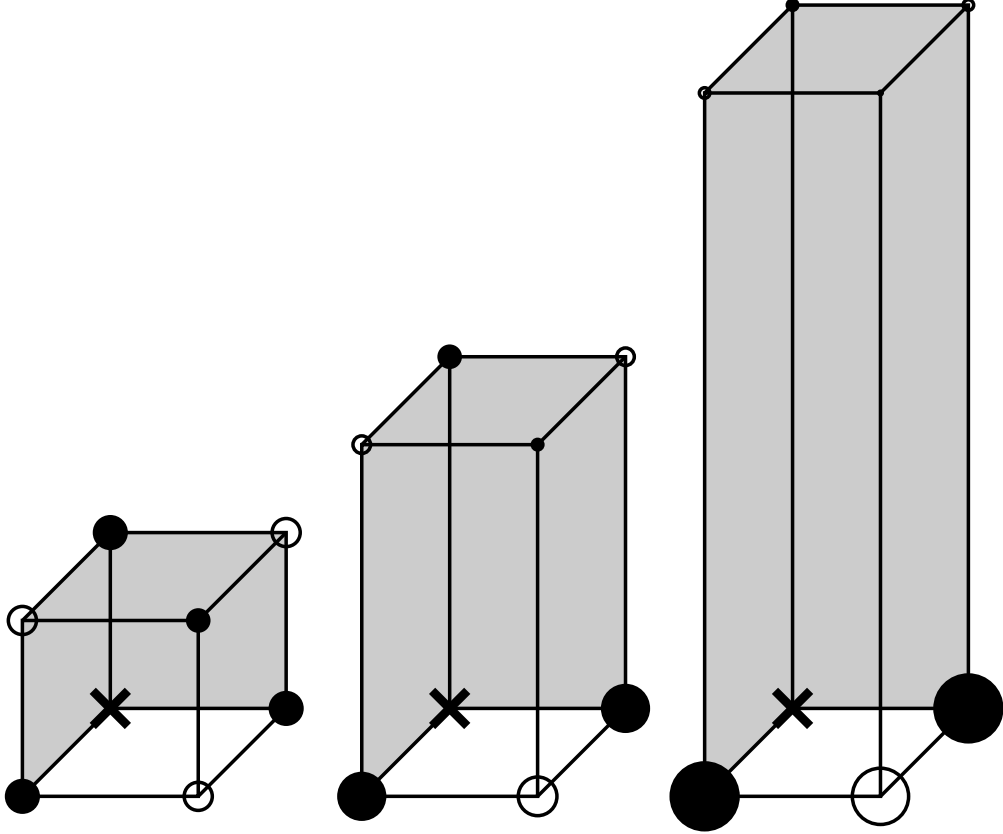


FIG. 10. The pairing potential for $\mathbf{q}_0 = [\pi, \pi, \pi]$ seen by a quasiparticle in a spin-singlet d_{xy} Cooper pair state given that the other quasiparticle is at the origin (marked by a cross). The figure depicts the evolution of the potential as one goes from a cubic to a tetragonal lattice by varying the parameter α_d . Closed circles denote repulsive sites and open circles attractive ones. The size of the circle is a measure of the strength of the interaction. The nodal planes of the d_{xy} state are represented by the shaded region.

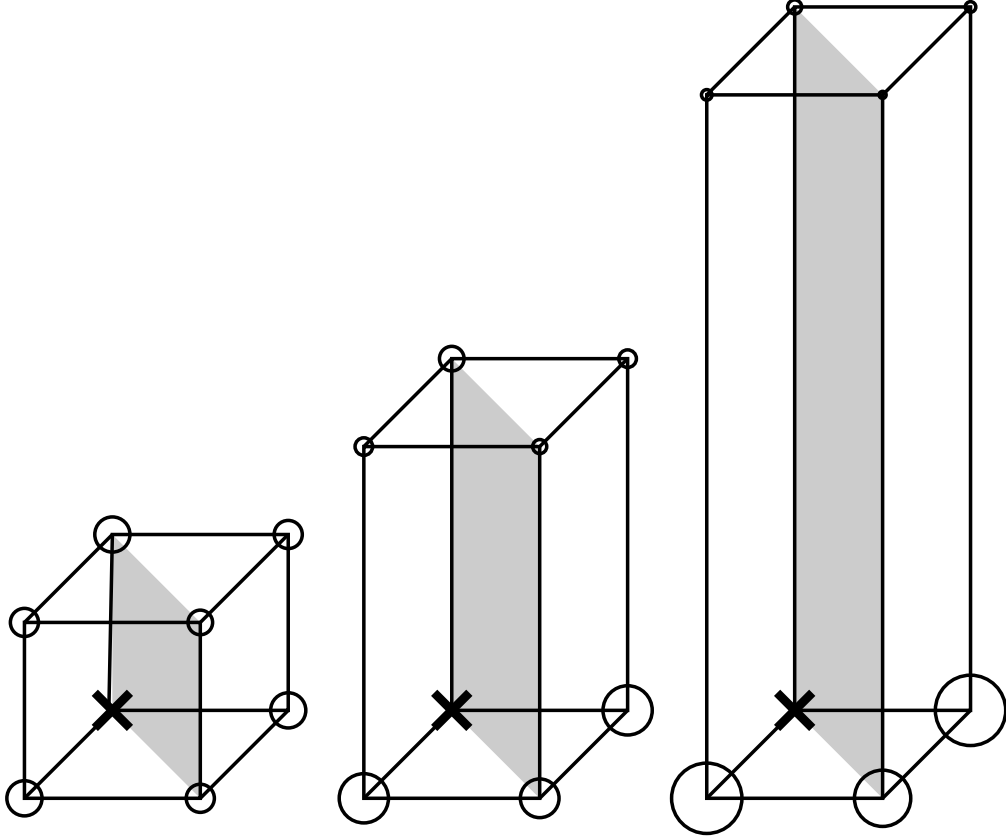


FIG. 11. The pairing potential for $\mathbf{q}_0 = [\pi/4, 0, 0]$ seen by a quasiparticle in a spin-singlet $d_{x^2-y^2}$ Cooper pair state given that the other quasiparticle is at the origin (marked by a cross). The figure depicts the evolution of the potential as one goes from a cubic to a tetragonal lattice by varying the parameter α_d . Open circles denote attractive sites. The size of the circle is a measure of the strength of the interaction. The nodal plane of the $d_{x^2-y^2}$ state is represented by the shaded region.